

LAYERED SILICATE / POLYPROPYLENE NANOCOMPOSITES

**A Thesis submitted to
the Graduate School of Engineering and Science of
Izmir Institute of Technology
in Partial Fulfillment of the Requirements for the Degree of
MASTER OF SCIENCE
in Mechanical Engineering**

**by
Kıvanç IŞIK**

**July 2006
Izmir, Turkey**

We approve the thesis of **Kıvanç IŞIK**

Date of Signature

.....

10 July 2006

Assoc. Prof. Dr. Metin TANOĞLU
Supervisor
Department of Mechanical Engineering
Izmir Institute of Technology

.....

10 July 2006

Assoc. Prof. Dr. Funda TIHMINLIOĞLU
Department of Chemical Engineering
Izmir Institute of Technology

.....

10 July 2006

Assoc. Prof. Dr. Sacide ALSOY ALTINKAYA
Department of Chemical Engineering
Izmir Institute of Technology

.....

10 July 2006

Assoc. Prof. Dr. Salih OKUR
Co-Supervisor
Department of Physics
Izmir Institute of Technology

.....

10 July 2006

Assoc.Prof.Dr. Talal SHAWAN
Department of Chemistry
Izmir Institute of Technology

.....

10 July 2006

Assoc. Prof. Dr. Barış ÖZERDEM
Head of Department
Izmir Institute of Technology

.....

Assoc. Prof. Dr. Semahat Özdemir
Head of the Graduate School

ACKNOWLEDGEMENTS

I am very grateful to Assoc.Prof.Dr. Metin Tanođlu for his supervision, guidance and encouragement during this study. I 'd like to thank to Assoc.Prof.Dr. Funda Tıhmınlıođlu for her valuable comments, recommendations and support. I acknowledge Ak Plastik San.Tic.Ltd.đti. for their support and specially I wish to thank my father, Aydın Iđık, for his continuous support and thoughtful advice to overcome difficulties. I also thank to my friends in IZTECH Centre of Material Research for their kind help in characterization studies. I'd like to express my heartfelt gratitude to dear family for their encouragement and understanding that enabled me to overcome the obstacles I faced during my study. Finally, I am grateful to my friends for assisting me in my research. Especially I wish to thank to Elçin Dilek Kaya and Emrah Bozkurt for their friendly motivation in every moment of my study.

ABSTRACT

LAYERED SILICATE / POLYPROPYLENE NANOCOMPOSITES

Layered silicate nanocomposites are new generation materials that have unique properties obtained by low particulate loadings. In this study, layered silicate/polypropylene nanocomposites were prepared by melt intercalation method. Homopolymer PP alone and maleic anhydride-grafted polypropylene (PPgMA) as a compatibilizer were used as the matrix. Clay (Na^+ montmorillonite, MMT) particles were used with and without structural modification to obtain silicate nano-layers within the PP matrix. Structural modification of MMT using hexadecyltrimethyl ammonium chloride (HTAC) was applied to obtain organophilic silicates (OMMT). XRD results demonstrated that the dispersion of the modified silicate layers and compatibilized with PPgMA (OMMT/PPgMA) is better than those for incompatibilized compositions. The addition of silicate layers increased the crystallization temperature of PP as well as the thermal stability, but the melting temperature of the nanocomposites was decreased by the addition of silicate as compared with neat PP. The mechanical characterizations exhibited an increase of 62% on tensile modulus and 15% on tensile stress at break as compared to neat PP due to the improved dispersion of silicate layers within PP in 3 wt.% OMMT/PPgMA/PP nanocomposites. The effect of clay modification and PPgMA compatibilization on the light transmission of PP nanocomposites was characterized by optical transmission analysis. For the OMMT/PPgMA/PP nanocomposites, light transmission was improved as the dispersion was enhanced. The flammability results demonstrated that unmodified MMT and modified OMMT decreased the burning rate of PP nanocomposites. The organic modification of clay and compatibilization decreased the rate of flammability. A decrease of 26% on the burning rate of PP was recorded in 10%wt. OMMT/PPgMA/PP nanocomposites.

ÖZET

TABAKALI SİLİKA / POLİPROPİLEN NANOKOMPOZİTLERİ

Tabakalı silikat nanokompozitleri, düşük kil ilavesinde çok iyi özellikler gösteren yeni nesil kompozit malzemelerdir. Bu çalışmada tabakalı silikat/polipropilen nanokompozitleri eriyik interkalasyon metodu ile hazırlanmıştır. Polipropilen ve maleik anhidrit aşılansmış polipropilen (PPgMA) matriks olarak kullanılmış, kil dolgusu (Na^+ montmorillonit, MMT) hem doğal olarak hem de yüzey modifikasyonu işleminden geçirilerek eriyik termoplastik içine ilave edilmiştir. Organik kil (OMMT), sodyum-iyonlu montmorillonitin hegzadesil trimetil amonyum klorit tuzu ile iyon yer değiştirme reaksiyonu yoluyla hazırlanmıştır. Organokilin ve nanokompozitlerin nano yapıları X-Işını Kırınımı metodu ile karakterize edilmiştir. %3,5 ve 10 MMT, OMMT ve OMMT/PPgMA kil içeren PP nanokompozitleri hazırlanmış, ileri XRD analizleri ile yüzey modifikasyonunun ve PPgMA ilavesinin kil tabakalarının matriks içerisindeki dağılımı incelenmiştir. XRD sonuçlarında modifiye kil tabakalarının, PPgMA içeren matriks yapısında dağılımının iyileştiği gözlenmiştir. Taramalı elektron mikroskobu (SEM) çalışmaları, modifikasyon işlemlerinin tabakaların daha iyi dağılmasını sağladığını ve kırılmanın gevreksi bir davranış gösterdiğini ortaya koymuştur. DSC analizlerinde kil ilavesinin PP'nin kristalizasyon sıcaklığını arttırdığı, fakat bunun yanında erime sıcaklığını düşürdüğü tespit edilmiştir. Organokil ilavesi ve PPgMA katkısı ile dağılımın iyileştirilmesi nanokompozitlerin termal bozunma sıcaklıklarını attırmıştır. Nanokompozitlerin çekme deneyleri yapılarak kil ilavesinin ve PPgMA modifikasyonunun mekanik değerlere etkisi incelenmiştir. %3 OMMT/PPgMA/PP nanokompozit yapısının çekme mukavemetinde %62 ve kopmada mukavemet değerinde %15'lik gelişmeler kaydedilmiştir. Polipropilen endüstride ambalaj malzemesi olarak kullanıldığı için optik özellikleri önem taşımaktadır. Üretilen nanokompozitlerin optik geçirgenlik analizleri yapılmıştır. 700 nm'de ışık geçirgenliğinin kilin modifikasyonu ve PPgMA ile iyileştiği tespit edilmiştir. %10 MMT-OMMT-OMMT/PPgMA nanokompozit örneklerinin atmosferik şartlarda UL-94 yanıcılık testiyle yanma hızları ve yanma zamanları ölçülmüştür. Kil ilavesi malzemelerin yanma hızını azaltmış, modifikasyon ve PPgMA katkısı bu malzemelerin yanma hızını %26 oranında gerilemiştir.

TABLE OF CONTENTS

LIST OF FIGURES	viii
LIST OF TABLES	xi
CHAPTER 1. INTRODUCTION	1
CHAPTER 2. NANOCOMPOSITES	4
2.1. Structure of Layered Silicates	6
2.2. Organically Modified Layered Silicates	7
2.3. Microstructure of Nanocomposites.....	10
2.4. Production of Nanocomposites	11
2.4.1. Solution Method	11
2.4.2. In-situ Polymerization Method	11
2.4.3. Melt Intercalation.....	12
2.5. Characterization of Nanocomposites	13
2.6. Properties of Nanocomposites	15
2.6.1. Layered Silicate/Epoxy Nanocomposites	15
2.6.2. Layered Silicate/Polyurethane Nanocomposites	16
2.6.3. Layered Silicate/Vinyl Polymer Nanocomposites.....	17
2.6.4. Layered Silicate/Polystyrene Nanocomposites.....	18
2.6.5. Specialty Polymer Nanocomposite Systems.....	18
2.6.6. Biodegradable Polymer Nanocomposite Systems	19
2.6.7. Polyolefin Nanocomposite Systems	19
2.6.7.1. Effect of Compatibilizer on the Properties of Polypropylene Nanocomposites	21
2.6.7.2. Thermal Properties of Polypropylene Nanocomposites	32
2.6.8. Other Properties of Nanocomposites	35
2.6.8.1. Gas Barrier Properties	35
2.6.8.2. Fire Retardant Properties	36
2.6.8.3. Optical Properties	37
2.6.8.4. Biodegradability.....	37

2.7. Modeling of Nanocomposites.....	40
2.7.1. Semi Empirical Predictions for Non-spherical Particulate Systems	42
2.7.1.1. Guth Model.....	42
2.7.1.2. Brodnyan Model	43
2.7.1.3. Halpin-Tsai (HT) Method.....	43
2.7.1.4. Modified Halpin-Tsai Model.....	44
 CHAPTER 3. EXPERIMENTAL.....	45
3.1. Materials	45
3.2. Organic Modification of Clay.....	45
3.3. Compatibilization of Organoclay with PPgMA.....	46
3.4. Production of Layered Silicate/Polypropylene Nanocomposites	46
3.5. Characterization of Nanocomposites	48
3.5.1. X-ray Diffraction Analysis	48
3.5.2. Scanning Electron Microscopy (SEM).....	49
3.5.3. Tensile Behavior of	49
3.5.4. Thermal Behavior of Nanocomposites	49
3.5.5. Optical Property Characterization	49
3.5.6. Flammability of Nanocomposites.....	50
 CHAPTER 4. RESULTS AND DISCUSSION	52
4.1. Microstructure of Nanocomposites.....	52
4.2. Tensile Properties of Nanocomposites	57
4.2.1. Model Predictions of Tensile Modulus of Nanocomposites.....	61
4.2.1.1. MMT/PP Nanocomposites.....	61
4.2.1.2. OMMT/PP Nanocomposites.....	63
4.3. Thermal Characterization	65
4.4. Optical Property	70
4.5. Flammability Behavior	72
 CHAPTER 5. CONCLUSION.....	74
 REFERENCES	76

LIST OF FIGURES

Figure 2.1. Schematic Illustration of 2:1 phyllosilicates structure and its SEM Image	7
Figure 2.2. Ion Exchange Reaction between Na-MMT and Alkyl Ammonium Molecules	8
Figure 2.3. Alkyl chain aggregation models: Open circles represent the CH ₂ segments while cationic head groups are represented by filled circles.....	10
Figure 2.4. Three main morphology achievable in nanocomposite structure	11
Figure 2.5. Microstructural Development during Melt Intercalation Process.....	12
Figure 2.6. (a) WAXD patterns, (b) TEM images of three different types of nanocomposites.....	14
Figure 2.7. (a) Compressive yield strength and (b) moduli for the pristine epoxy polymer and the exfoliated epoxy– clay nanocomposites prepared from three different kinds of organoclays	16
Figure 2.8. Stress–strain curves for (a) a pristine polyurethane elastomer; (b) a polyurethane–clay nanocomposite prepared from organomontmorillonite 5 wt.%	17
Figure 2.9. Yield stress (a) and Young’s modulus (b) of unfilled PP and PPLSNs as a function of organoclay contents at constant loading of antioxidant, 0.5 phr	22
Figure 2.10. Tensile Strength of PP Nanocomposites.....	23
Figure 2.11. Tensile Modulus of PP Nanocomposites	23
Figure 2.12. Izod Impact Strength of PP Nanocomposites	23
Figure 2.13. Mechanical Properties of PP Nanocomposites	25
Figure 2.14. Tensile Modulus of PP Nanocomposites	28
Figure 2.15. Flexural Modulus of PP Nanocomposites	29
Figure 2.16. Impact Strength of PP Nanocomposites	29
Figure 2.17. Formation of tortuous path in polymer layered silicate nanocomposites.....	36
Figure 2.18. UV transmittance spectra of PVA and PVA/MMT nanocomposites 4 and 10 wt% MMT.....	37

Figure 2.19. Biodegradability of APES nanocomposites with: (a) Cloisite 30B and (b) Cloisite 10A	38
Figure 2.20. Real picture of biodegradability of neat PLA and PLACN4 with time	39
Figure 2.21. Time dependence of residual weight, R_w and M_w of PLA and PLACN4 at $58 \pm 2^\circ\text{C}$	39
Figure 3.1. Processing Stages of Organic Modification of Clay	46
Figure 3.2. Processing Stages for clay/PP Nanocomposites	47
Figure 3.3. Two-roll compounding mixer	47
Figure 3.4. Hot Press	48
Figure 3.5. Hollow Die Punch and Sample Cutter	48
Figure 3.6. UL94 Horizontal burn set up for flammability testing	50
Figure 4.1. XRD Patterns of MMT and OMMT	52
Figure 4.2. XRD Pattern of Neat PP	53
Figure 4.3. XRD Patterns of MMT/PP Nanocomposites	53
Figure 4.4. XRD Patterns of PPgMA Compatibilized MMT/PP Nanocomposites	54
Figure 4.5. XRD Patterns of OMMT/PP Nanocomposites	54
Figure 4.6. XRD Patterns of PPgMA Compatibilized OMMT/PP Nanocomposites	55
Figure 4.7. Effect of PPgMA compatibilization and clay surface modification on XRD Patterns of PP Nanocomposites for 10 wt.% of clay loadings	56
Figure 4.9. Fractured surface SEM images of (a) neat PP and (b) 5 wt.% MMT/PP Nanocomposite	57
Figure 4.10. Fractured surface SEM images of (a) 5 wt.% OMMT/PP and (b) 5 wt.% OMMT/PPgMA/PP	57
Figure 4.11. Tensile modulus as a function of clay loading for clay/PP nanocomposites	59
Figure 4.12. Tensile strength as a function of clay loading for clay/PP nanocomposites	59
Figure 4.13. Tensile Stress at Break as a function of clay loading for clay/PP nanocomposites	60

Figure 4.14. % Elongation at Yield as a function of clay loading for clay/PP nanocomposites.....	60
Figure 4.15. Predicted E_c vs. V_f values for MMT/PP Nanocomposites based on: (a) Guth , (b) Halpin-Tsai , (c) Modified Halpin-Tsai and (d) Brodnyan Models	62
Figure 4.16. Predicted E_c vs. V_f values for MMT/PP Nanocomposites based on: (a) Guth , (b) Halpin-Tsai , (c) Modified Halpin-Tsai , (d) Brodnyan Models with the best fit of $\alpha = 11$	63
Figure 4.17. Predicted E_c vs. V_f values for OMMT/PP Nanocomposites based on: (a) Guth , (b) Halpin-Tsai , (c) Modified Halpin Tsai , (d) Brodnyan Models	64
Figure 4.18 Predicted E_c vs. V_f values for OMMT/PP Nanocomposites based on : (a) Guth , (b) Halpin-Tsai , (c) Modified Halpin-Tsai and (d) Brodnyan Models with the best fit of $\alpha = 11$	65
Figure 4.19. (a) Melting Behaviour (Heating) and (b) Crystallization Behaviour (Cooling) Curves of MMT/PP, OMMT/PP and OMMT/PPgMA/PP nanocomposites.....	66
Figure 4.20. DSC thermograms showing the thermal degradation behaviour of (a) OMMT/PP and (b) OMMT/PPgMA/PP Nanocomposites.....	68
Figure 4.21. MMT/PP, OMMT/PP and OMMT/PPgMA/PP Nanocomposites	70
Figure 4.22. Light Transmission spectra for MMT/PP, OMMT/PP and OMMT/PPgMA/PP Nanocomposites measured with UV-VIS light spectroscopy	71
Figure 4.23. Clay/ PP nanocomposites in UL-94 testing	72
Figure 4.24. Burning rate of neat PP and nanocomposites prepared with PP and 10 wt.% of MMT, OMMT and OMMT/PPgMA.....	73
Figure 4.25. Burning Time of neat PP and nanocomposites prepared with PP and 10 wt.% of MMT, OMMT and OMMT/PPgMA	73

LIST OF TABLES

Table 2.1.	Mechanical Properties of Compatibilized Nanocomposites	25
Table 2.2.	Mechanical Properties of DEM Compatibilized PP/Clay Nanocomposites.....	30
Table 2.3.	Mechanical Properties of MA Compatibilized PP/Clay Nanocomposites.....	31
Table 3.1.	The Properties and suppliers of the raw materials used in the study.....	45
Table 4.1.	Tensile Modulus of the nanocomposites as a function of volume fractions	61
Table 4.2.	Material data used in the modelling study.....	61
Table 4.3.	Melting(T_m) and crystallization temperatures(T_c) of neat PP and silicate/PP nanocomposites.....	67
Table 4.4.	Degradation temperature of neat PP and silicate/PP nanocomposites.....	69

CHAPTER 1

INTRODUCTION

Polymers with particulate fillers have wide industrial applications to improve the stiffness and toughness of polymers, to enhance their barrier properties and their resistance to fire and ignition. Addition of particulate fillers sometimes results in undesired properties such as brittleness or opacity. Nanocomposites are a new class of composites that are particle-filled composites in which at least one dimension of the dispersed particles is in the nanometer range. One of the interesting aspects of the use of nanofillers is the low concentration of that filler that needs to be added to the polymer system to obtain desired property improvements.

Layered silicate/polymer nanocomposites were first reported in 1950 as a patent literature (Carter et al. 1950). However, it was not popular until Toyota researchers began a detailed experimentation in the year of 1996 on the nylon 6/clay nanocomposites (Usuki et al. 1993, 1995). In recent years, nanocomposites received a great interest in academic, governmental and industrial studies (Usuki et al. 1993, 1995).

The improvements in thermal, mechanical and flammability properties of clay/polymer nanocomposites are significantly higher than those achieved in traditional filled polymers. Up to now, these systems have experienced some success for several kinds of polar polymers. However, for polymers with low polarity, such as polyolefins, the improvements are not very significant due to the low compatibility between the clay and the polyolefins.

One of the most commonly used organophilic layered silicates is derived from montmorillonite (MMT). Its structure is made of several stacked layers, with a layer thickness between 1.2-1.5 nm and a lateral dimension of 100– 200 nm (Marchant et al. 2002, Moore et al. 1997). These layers organize themselves to form the stacks with a regular gap between them, called interlayer or gallery. The sum of the single layer thickness and the interlayer represents the repeat unit of the multilayer material, called d-spacing or basal spacing (d_{001}), and is calculated from the (001) harmonics obtained from X-ray diffraction patterns. The clay is naturally a hydrophilic material, which makes it difficult to exfoliate in a polymer matrix. Therefore, the surface treatment of

silicate layers is necessary to render its surface more hydrophobic, which facilitates exfoliation. Generally, this can be done by ion-exchange reactions with cationic surfactants, including primary, secondary, tertiary and quaternary alkylammonium cations (Fornes 2002, Le Pluart 2002). This modification also leads to expand the basal spacing between the silicate layers due to the presence of alkyl chain intercalated in the interlayer and to obtain organoclay (OMMT).

Polypropylene (PP) is one of the most widely used plastics in large volume. To overcome the disadvantages of PP, such as low toughness and low service temperature, researchers have tried to improve the properties with the addition of nanoparticles that contains polar functional groups. An alkylammonium surfactant has been adequate to modify the clay surfaces and promote the formation of nanocomposite structure. Until now, two major methods, i.e., in-situ polymerization (Ma et al. 2001, Pinnavaia 2000) and melt intercalation (Manias et al. 2001) have been the techniques to prepare clay/PP nanocomposites. In the former method, the clay is used as a catalyst carrier, propylene monomer intercalates into the interlayer space of the clay and then polymerizes there. The macromolecule chains exfoliate the silicate layers and make them disperse in the polymer matrix evenly. In melt intercalation, PP and organoclay are compounded in the molten state to form nanocomposites.

As the hydrophilic clay is incompatible with polypropylene, compatibilization between the clay and PP is necessary to form stable PP nanocomposites. There are two ways to compatibilize the clay and PP. In the first approach, the enthalpy of the interaction between the surfactant and the clay is reduced. In the second approach, a compatibilizer, such as maleic anhydride grafted PP (PPgMA) can be used (Manias et al. 2001). The clay is melt compounded with the more polar compatibilizer to form an intercalated master batch. The master batch is then compounded with the neat PP to form the PP nanocomposite. In this way, the PPgMA pretreated OMMT is dispersed uniformly in the PP matrix. The shear force during compounding or extruding plays an important role in determining the structure of the nanocomposite. As a result, the properties of the resulting hybrid materials depend strongly on the processing conditions. Okada et al. (1997), Kato et al. (1997) and Hasegawa et al. (1997) showed that there are two important factors to achieve the exfoliation of the layered silicates; (1) the compatibilizer should be miscible with the polypropylene matrix, and (2) it should include a certain amount of polar functional groups in a molecule. Generally, the PPs

modified with maleic anhydride (MA) fulfill these two requirements and are frequently used as compatibilizer for polypropylene nanocomposites.

The amount of grafting percentage of PPgMA used in the literature is typically 0.5–2% found in literature to produce polypropylene nanocomposites. Low concentration of PPgMA has been found not to enhance the compatibility greatly, while PPgMA with excess concentration tends to cause deterioration of the properties of the nanocomposite due to the low molecular weight of the PPgMA. Generally, to achieve a significant intercalation and improvement on the property, an optimum value of grafted polymer/organoclay ratio is required. Typically, the ratio of 3:1 has been found the best sorted to achieve the effective intercalation and the highest performance (Lopez et al. 2003, Morgan et al. 2003).

The optical properties of polypropylene composites are important especially for commercial packaging purposes. The layers of 1 nm thickness dispersed in polymer matrix allow producing plastic films with optical clarity. The exfoliated nanosilicate layers generate a tortuous path for oxygen and water vapour penetration of the neat polymers especially for polyolefins like polyethylene and polypropylene. This is a very important property for increasing the shelf life of food with durable packaging.

In this study, PP based nanocomposites containing various content of MMT and organo-modified OMMT were prepared by melt intercalation with and without a compatibilizer (PPgMA). The effects of modification of the clay particles and compatibilization of filler/matrix interface on the morphology and the properties of nanocomposites were investigated. The microstructural features were characterized by scanning electron microscopy (SEM) and X-ray diffraction (XRD) techniques. Mechanical properties, thermal behaviour, flame retardancy and optical properties of the prepared nanocomposites were investigated within the present research.

CHAPTER 2

NANOCOMPOSITES

Layered silicates dispersed as reinforcing phase in an engineering polymer matrix are one of the most important forms of such ‘‘hybrid organic–inorganic nanocomposites’’. Although the high aspect ratio of silicate nanolayers is ideal for reinforcement, the nanolayers do not easily disperse in the most polymers due to their preferred face-to-face stacking in agglomerated tactoids. Dispersion of the tactoids into discrete monolayers is further hindered by the intrinsic incompatibility of hydrophilic-layered silicates and hydrophobic engineering plastics.

Work in polymer nanocomposites has exploded over the last few years. The prospect of a new materials technology that can function as a low-cost alternative to high-performance composites for applications ranging from automotive to food packaging to tissue engineering has become irresistible to researchers around the world.

The essence of nanotechnology is the ability to work at the molecular level to create large structures with fundamentally new molecular organization. Materials with features on the scale of nanometers often have properties different from their macro scale counterparts. Important among nanoscale materials are nanohybrids or nanocomposites, materials in which the constituents are mixed on a nanometer-length scale. They often exhibit properties superior to conventional composites, such as strength, stiffness, thermal and oxidative stability, barrier properties, as well as unique properties like self-extinguishing behavior and tunable biodegradability (Krishnamoorti, 2001).

Polymer/layered silicate nanocomposites are a new class of composite materials where inorganic silicates, zeolites and clays having nano-scale dimensions are dispersed in polymeric matrix (Motomatsu, Takahashi, 1997; Frisch, Mark, 1996; Usuki, Kawasumi, 1993). They often exhibit remarkable improvement in materials properties as compared with virgin polymer or conventional micro and macro-composites.

Advancements in material performance depend on the ability to synthesize new materials that exhibit enhanced properties, such as strength, fracture toughness, impact resistance, durability, decreased flammability and gas permeability, etc. Polymer/layered silicate nanocomposites are ideal materials to meet this challenge, as it

has been shown that they have the potential to deliver the improved properties with minimal increase in weight. It is important that the degree of enhancement of a particular property is highly dependent on the matrix/filler system used, the extent of filler adhesion to the matrix, and the level of dispersion of the filler throughout the matrix.

Silicates are the most popular materials used in the synthesis of polymer nanocomposites. They are composed of layers that have one dimension in nano-scale. The most common nanofiller is sodium montmorillonite, i.e. a natural smectite clay (2:1 phyllosilicate) that consists of regular stacks of aluminosilicate layers with a high aspect ratio and a high surface area. Because of the hydrated sodium cations in the clay galleries, natural montmorillonite is hydrophilic, which is a major drawback to have it homogeneously dispersed in organic polymers. The penetration of polymer or monomer molecules into the silicate galleries in the nanocomposite system determines the homogeneity of the clay dispersion by breaking up the layered structure. The wetting of particle surfaces by organic polymers is very difficult due to this organophobic behavior of the natural clay. This may be overcome by the modification of clay with surfactants including onium ions. In this modification, a cation exchange reaction takes place between the metal cations in the galleries and the surfactant onium ions. The intercalation of interlayer spacing between silicate galleries occurs within organophilic clays due to the modification. This improves the diffusion of monomer and polymer molecules into the silicate galleries effectively during polymer/layered silicate nanocomposite synthesis.

Although the intercalation chemistry of polymers when mixed with appropriately modified layered silicate and synthetic layered silicates has long been known (Blumstein 1965, Theng 1979), the field of polymer/layered silicate nanocomposites has become popular recently. Two major findings have stimulated the revival of interest in these materials. In the first report from the Toyota research group for a Nylon-6 (P6)/montmorillonite (MMT) nanocomposite (Usuki et al. 1990), in which very small amounts of layered silicate loadings, the results pronounced improvements in thermal and mechanical properties. The second was the observation by Vaia et al. (Vaia et al. 1993) that it is possible to melt-mix polymers with layered silicates without the use of organic solvents.

Exfoliated or delaminated structures result from the complete and uniform dispersion of the individual silicate layers in a continuous polymer matrix. Melt

intercalation of preformed polymers and in situ intercalative polymerization are the two techniques that are most commonly used to prepare polymer/clay nanocomposites.

The first method is effective whenever the thermodynamics of the melted polymer/organoclay pair allows the chains to crawl within the clay interlayer spaces, so pushing the individual sheets apart one from each other. The second method relies on the swelling of the organoclay by the monomer, followed by the in situ polymerization initiated thermally or by addition of a suitable compound. The chain growth in the clay galleries triggers the clay exfoliation and the nanocomposite formation.

It is important to build an understanding that will permit the prediction and control of nanocomposite properties. As an example it is known that nanocomposites based on nylon and clays can attain significant improvements in stiffness, strength and heat distortion temperature with much lower inorganic content as compared to corresponding macro composites, making them lightweight as well. This combination of enhanced performance and reduced weight contribute to more fuel efficient and environmentally friendly automobiles.

2.1. Structure of Layered Silicates

Layered silicates dispersed as a reinforcing phase in polymer matrix are one of the most important forms of hybrid organic-inorganic nanocomposites (Okada and Usuki, 1995). Their crystal structure consists of layers made up of two tetrahedrally coordinated silicon atoms fused to an edge-shared octahedral sheet of either aluminum or magnesium hydroxide. The layer thickness is around 1 nm, and the lateral dimensions of these layers may vary from 30 nm to several microns or larger, depending on the particular layered silicate. Van der Waals forces stack the layers leading to a regular gap named as interlayer or gallery.

MMT, hectorite, and saponite are the most commonly used layered silicates. Layered silicates have two types of structure: tetrahedral-substituted and octahedral substituted. In the case of tetrahedrally substituted layered silicates the negative charge is located on the surface of silicate layers, and hence, the polymer matrices can interact more readily with these than with octahedrally-substituted material. The structure and chemistry for these layered silicates are shown in Figure 2.1.(Süd-Chemie, 2000).

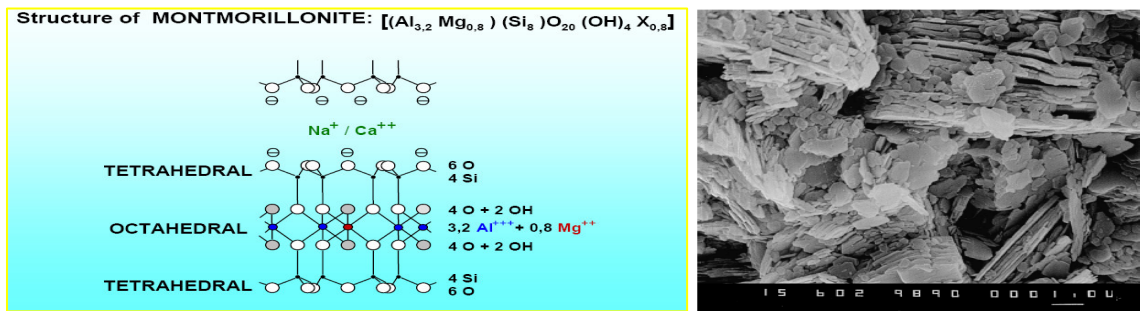


Figure 2.1. Schematic Illustration of 2:1 phyllosilicates structure and its SEM Image
(Source: WEB_1 2000)

There are two particular characteristics of layered silicates that are generally considered for polymer/layered silicate nanocomposites. The first is the ability of the silicate particles to disperse into separate layers. The second is the ability to modify their surface chemistry through ion exchange reactions with organic and inorganic cations. These two characteristics are related to each other since the degree of dispersion of layered silicate in a particular polymer matrix depends on the interlayer cation.

2.2. Organically Modified Layered Silicates

Nanocomposite synthesis may not be successful with a physical mixture of polymer and layered silicate. In immiscible systems, conventionally filled polymers, the poor physical interaction between the organic and the inorganic components leads to poor mechanical and thermal properties. In contrast, strong interactions between the polymer and the layered silicate in polymer/layered silicate nanocomposites lead to the organic and inorganic phases being dispersed at the nanometer level. As a result, nanocomposites exhibit unique properties not shared by their micro counterparts or conventionally filled polymers (Usuki et al. 1990, Biswas et al. 2001).

Pristine layered silicates usually contain hydrated Na⁺ or K⁺ ions (Brindly et al. 1980). Obviously, in this pristine state, layered silicates are only miscible with hydrophilic polymers, such as poly(ethylene oxide) (PEO) (Aranda et al. 1992), or poly(vinyl alcohol) (PVA) (Greenland 1963). To render layered silicates miscible with other polymer matrices, one must normally convert the hydrophilic silicate surface to an organophilic one, making the intercalation of many engineering polymers possible.

Generally, this can be done by ion-exchange reactions with cationic surfactants including primary, secondary, tertiary, and quaternary alkylammonium or alkylphosphonium cations. Alkylammonium or alkylphosphonium cations in the organosilicates lower the surface energy of the inorganic host and improve the wetting characteristics of the polymer matrix, and result in a larger interlayer spacing. Additionally, the alkylammonium or alkylphosphonium cations can provide functional groups that can react with the polymer matrix, or in some cases initiate the polymerization of monomers to improve the strength of the interface between the inorganic and the polymer matrix (Blumstein 1965, Krishnamoorti et al. 1996).

The replacement of inorganic exchange cations by organic onium ions on the gallery surfaces of smectite clays not only serves to match the clay surface polarity with the polarity of the polymer, but it also expands the clay galleries (Figure 2.2). This facilitates the penetration of the gallery space intercalation by either the polymer precursors or preformed polymer. Depending on the charge density of clay and the onium ion surfactant, different arrangements of the onium ions are possible. In general, the longer the surfactant chain length, and the higher the charge density of the clay, the further apart the clay layers will be forced. This is expected since both of these parameters contribute to increasing the volume occupied by the intra gallery surfactant. Depending on the charge density of the clay, the onium ions may lie parallel to the clay surface as a monolayer, a lateral bi-layer, a pseudo-tri-molecular layer, or an inclined paraffin structure. At very high charge densities, large surfactant ions can adopt lipid bi-layer orientations in the clay galleries. (Lagaly, 1986)

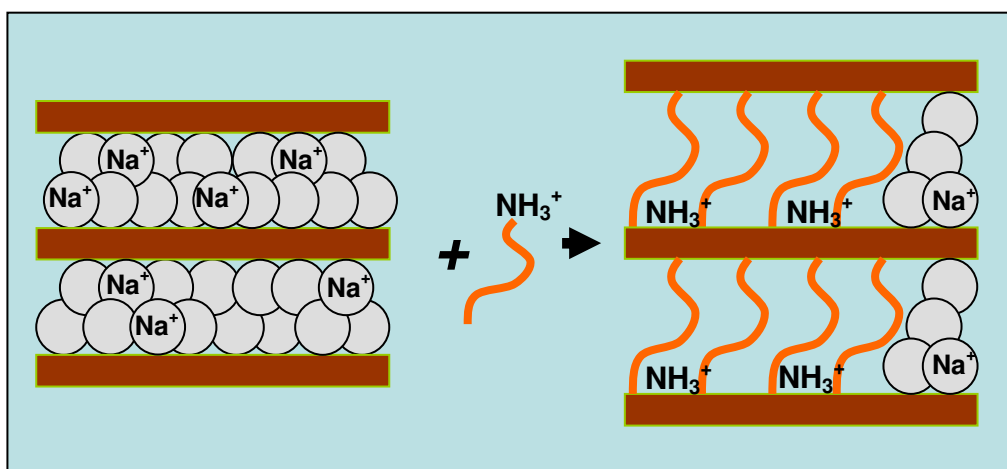


Figure 2.2. Ion Exchange Reaction between Na-MMT and Alkyl Ammonium Molecules

The orientations of onium ion chains in organoclay were initially deduced based on infrared and XRD measurements. More recent modeling experiments have provided further insights into the packing orientations of the alkyl chains in organically modified layered silicates.(Lagaly, 1986)

Molecular dynamics MD simulations were used to study molecular properties such as density profiles, normal forces, chain configurations and trans-gauche conformer ratios.(Vaia et al. 1993) For the mono, bi and pseudo-tri-layers with respective d-spacing of 13.2, 18.0 and 22.7 °A, a disordered liquid-like arrangement of chains was preferred in the gallery. In this disordered arrangement the chains do not remain flat, but instead, overlap and co-mingle with onium ions in opposing layers within the galleries. However, for the tri-layer arrangement, the methylene groups are primarily found within a span of two layers and only occasionally do they continue into the layer opposite to the positive head group. (Hackett et al., 1998)

As anticipated, the onium head group is also noted to reside nearer the silicate surface relative to the aliphatic portion of the surfactant. The highest preference conformer is trans over gauche for the maximum surfactant chain length just before the system progresses to the next highest layering pattern. This is expected since the alkyl chains must be optimally packed under such dense surfactant concentrations.(Pinnavaia, 1995)

Traditional structural characterization to determine the orientation and arrangement of the alkyl chain was performed using wide angle X-ray diffraction (WAXD). Depending on the packing density, temperature and alkyl chain length, the chains were thought to lie either parallel to the silicate layers forming mono or bi-layers, or radiate away from the silicate layers forming mono or bimolecular arrangements. (Lagaly,1986). The alkyl chains can vary from liquid-like to solid-like, with the liquid-like structure dominating as the interlayer density or chain length decreases (Figure 2.3), or as the temperature increases. There are three models for alkyl chain aggregation: (a) short chain lengths, the molecules are effectively isolated from each other, (b) medium lengths, quasi discrete layers form with various degree of in plane disorder and inter digitations between the layers and (c) long lengths, interlayer order increase leading to a liquid-crystalline polymer environment. This occurs because of the relatively small energy differences between the trans and gauche conformers; the idealized models described earlier assume all trans conformations. In addition, for

longer chain length surfactants, the surfactants in the layered silicate can show thermal transition akin to melting or liquid-crystalline to liquid-like transitions upon heating.

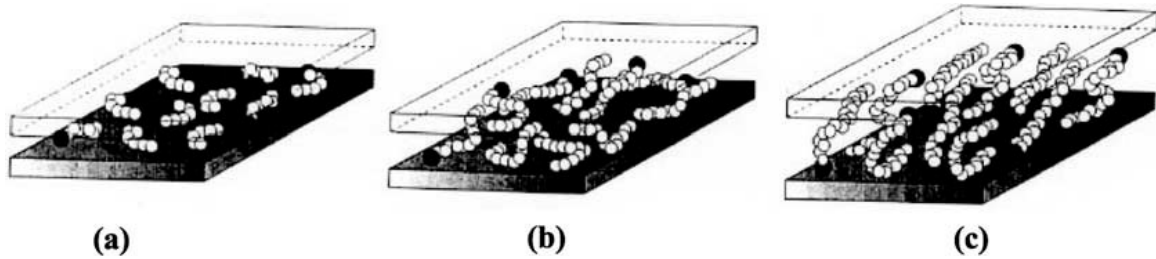


Figure 2.3. Alkyl chain aggregation models: Open circles represent the CH_2 segments while cationic head groups are represented by filled circles
(Source: Vaia et al., 1996).

2.3. Microstructure of Nanocomposites

Layered silicates have layer thickness with the order of 1 nm and a very high aspect ratio (e.g. 10–1000). A low weight percent of layered silicates that are properly dispersed throughout the polymer matrix thus create much higher surface area for polymer/filler interaction as compared to conventional composites. Depending on the surface properties, level of dispersion and the strength of interfacial interactions between the polymer matrix and layered silicate (modified or not), three different types of polymer/layered silicate composite microstructure are achievable (Figure 2.4).

a. Phase separated microcomposites: conceptually the unmodified silicate layers are stacked together and the polymer molecules cannot penetrate into the galleries. The silicates are a kind of fillers that stay as agglomerates.

b. Intercalated nanocomposites: in intercalated nanocomposites, the insertion of a polymer matrix into the layered silicate structure occurs in a crystallographically regular fashion, regardless of the clay to polymer ratio. Intercalated nanocomposites are normally interlayer by a few molecular layers of polymer.

c. Exfoliated nanocomposites: in an exfoliated nanocomposite, the individual clay layers are separated in a continuous polymer matrix by an average distances that depends on clay loading. Usually, the clay content of an exfoliated nanocomposite is much lower than those for an intercalated nanocomposite.

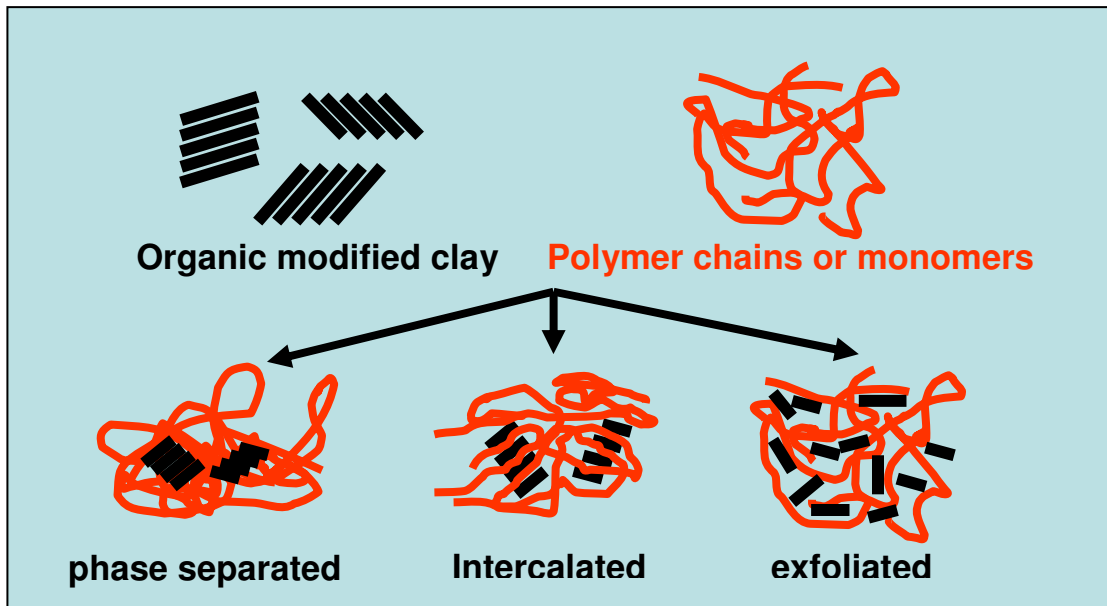


Figure 2.4. Three main morphology achievable in nanocomposite structure

2.4. Production of Nanocomposites

There are essentially some different approaches to synthesize polymer-clay nanocomposites: melt intercalation, solution and in-situ polymerization.

2.4.1. Solution Method

In the solution method, the organoclay and the polymer are dissolved in a polar organic solvent. The entropy gained by desorption of solvent molecules allows the polymer chains to diffuse between the clay layers, compensating for their decrease in conformational entropy. After evaporation of the solvent, an intercalated nanocomposite is formed. This strategy can be used to synthesize epoxy-clay nanocomposites but the large amount of solvent required is a major disadvantage (Ahmadi et al. 2004)

2.4.2. In-situ Polymerization Method

The in-situ polymerization approach was first developed by Toyota group to make Nylon-6 nanocomposites from caprolactam monomer. It has been applied to

several other systems, including epoxies and styrene. This technique was found to be the most effective one for a thermoset polymer matrix nanocomposite (Nigam et al. 2004). It is similar to the solution method except that the role of the solvent is replaced by a polar monomer solution. Nanoscale particles are dispersed in the monomer or monomer solution, and the resulting mixture is polymerized by standard polymerization methods (Qutubuddin et al. 2005). The polymerization is believed to be the indirect driving force of the exfoliation. The clay, due to its high surface energy, attracts polar monomer molecules in the clay galleries until equilibrium is reached. The polymerization reactions occurring between the layers lower the polarity of the intercalated molecules and displace the equilibrium. This allows new polar species to diffuse between the layers and progressively exfoliate the clay. Therefore, the nature of the curing agent as well as the curing conditions is expected to play a role in the exfoliation process (Kornmann et al. 2001).

2.4.3. Melt Intercalation

A thermoplastic polymer is melt mixed with organophilic clay at elevated temperatures (Figure 2.5). The polymer chains intercalates between the individual silicate layers of the clay. The proposed driving force of this mechanism is the enthalpic contribution of the polymer/organoclay interactions. This method is becoming increasingly popular since the resulting thermoplastic nanocomposites may be processed by conventional methods such as extrusion and injection molding (Ahmadi et al. 2004)

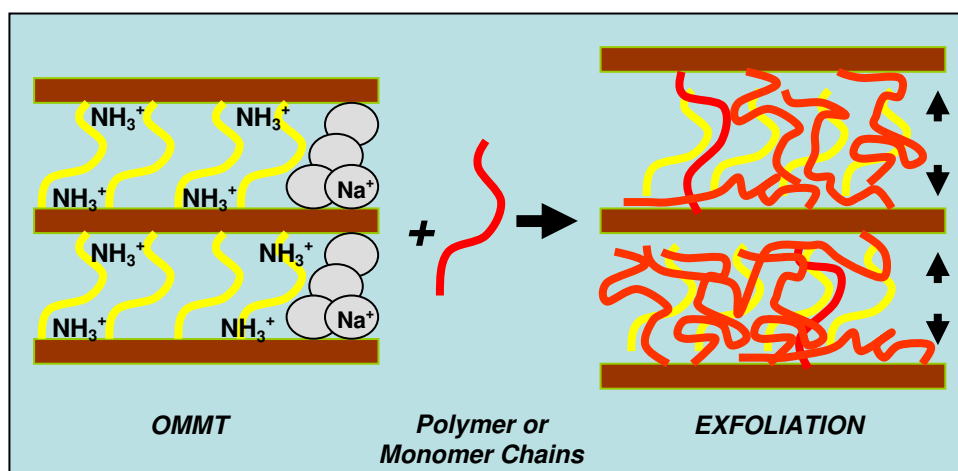


Figure 2.5. Microstructural Development during Melt Intercalation Process

2.5. Characterization of Nanocomposites

Generally, the structure of nanocomposites has typically been established using WAXD analysis and transmission electron micrographic (TEM) observation. Due to its easiness and availability WAXD is most commonly used to probe the nanocomposite structure (Giannelis 1996, Vaia et al. 1996) and occasionally to study the kinetics of the polymer melt intercalation (Vaia et al. 1996).

By monitoring the position, shape, and intensity of the basal reflections from the distributed silicate layers, the nanocomposite structure (intercalated or exfoliated) may be identified. For example, in an exfoliated nanocomposite, the extensive layer separation associated with the delamination of the original silicate layers in the polymer matrix results in the eventual disappearance of any coherent X-ray diffraction from the distributed silicate layers. On the other hand, for intercalated nanocomposites, the finite layer expansion associated with the polymer intercalation results in the appearance of a new basal reflection corresponding to the larger gallery height. Although WAXD offers a convenient method to determine the interlayer spacing of the silicate layers in the original layered silicates and in the intercalated nanocomposites (within 1–4 nm), little can be said about the spatial distribution of the silicate layers or any structural non-homogeneities in nanocomposites.

Additionally, some layered silicates initially do not exhibit well-defined basal reflections. Thus, peak broadening and intensity decreases are very difficult to study systematically. Therefore, conclusions concerning the mechanism of nanocomposites formation and their structure based solely on WAXD patterns are only tentative. On the other hand, TEM allows a qualitative understanding of the internal structure, spatial distribution of the various phases, and views of the defect structure through direct visualization. However, special care must be exercised to guarantee a representative cross-section of the sample. As an example, the WAXD patterns and corresponding TEM images of three different types of nanocomposites are presented for nylon 6/clay nanocomposites based on the study of Mathias et al., 1999 (Figure 2.6).

Both TEM and WAXD are essential tools for evaluating nanocomposite structure (Morgan et al. 2003). However, TEM is time intensive, and only gives qualitative information on the sample as a whole, while low angle peaks in WAXD allow quantification of changes in layer spacing. Typically, when layer spacing exceed

6–7 nm in intercalated nanocomposites or when the layers become relatively disordered in exfoliated nanocomposites, associated WAXD features weaken to the point of not being useful. However, recent simultaneous small angle X-ray scattering (SAXS) and WAXD studies yielded quantitative characterization of nanostructure and crystallite structure in PA6 based nanocomposites (Mathias et al. 1999). Very recently, Bafna et al. (Bafna et al. 2003) developed a technique to determine the three-dimensional (3D) orientation of various hierarchical organic and inorganic structures in a layered silicate/polymer nanocomposite. They studied the effect of compatibilizer concentration on the orientation of various structures in nanocomposites using 2D SAXS and 2D WAXD in three sample/camera orientations.

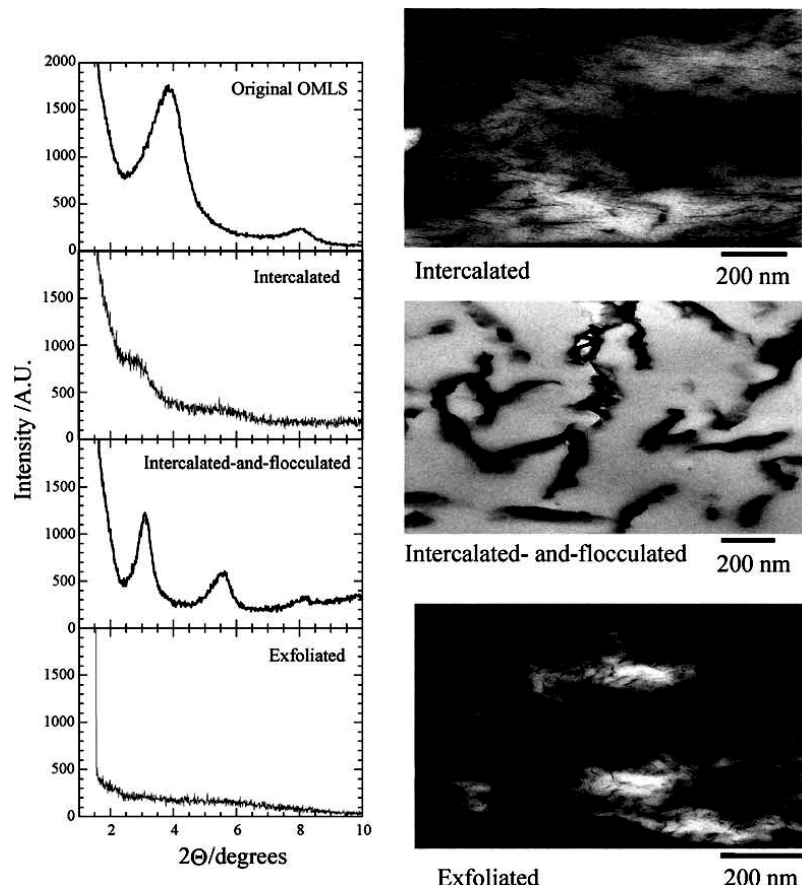


Figure 2.6. (a) WAXD patterns, (b) TEM images of three different types of nanocomposites. (Source: Mathias et al. 1999)

Reflections and orientation of six different structural features were easily identified: (a) clay clusters/tactoids (0.12 μm), (b) modified/intercalated clay stacking period (002) (24–31 Å), (c) stacking period of unmodified clay platelets (002) (13 Å),

(d) clay (110) and (020) planes, normal to (b) and (c), (e) polymer crystalline lamellae (001) ($190\text{--}260\text{ \AA}$), long period ((001) is an average crystallographic direction), and (f) polymer unit cell (110) and (200) planes.

2.6. Properties of Nanocomposites

Nanocomposites consisting of a polymer and layered silicate (modified or not) frequently exhibit remarkably improved mechanical and materials properties as compared to those of pristine polymers containing a small amount ($<5\text{ wt.}\%$) of layered silicate. Improvements include a higher modulus, increased strength and heat resistance, decreased gas permeability and flammability, and increased biodegradability of biodegradable polymers. The main reason for these improved properties in nanocomposites is the stronger interfacial interaction between the matrix and layered silicate, as compared with conventional filler-reinforced systems.

2.6.1. Layered Silicate/Epoxy Nanocomposites

Clay nanolayers have been shown to be very effective reinforcements in epoxy systems (Lan and Pinnavaia 1994; Messersmith and Giannelis 1994; Massam and Pinnavaia 1998). The key to achieve an exfoliated epoxy–clay nanocomposite structure is first to load the clay gallery with hydrophobic onium ions, and then expand the gallery region by diffusing in the epoxide, the curing agent or a mixture of the two. Interestingly, acidic onium ions catalyze intragallery polymerization at a rate that is competitive with extragallery polymerization. However, the relative rates of reagent intercalation, chain formation and network cross-linking have to be controlled in order to form the gel state and, eventually, the fully cured epoxy-exfoliated clay nanocomposite (Wang and Pinnavaia 1998). Aliphatic amine, aromatic amine, anhydride and catalytic curing agents all have been chosen to form an epoxy matrix with broad glass transition temperatures. However, the clay nanolayers are more effective in improving mechanical properties when the polymer is in its rubbery state vs. the glassy state. For instance, $7.5\text{ vol.}\%$ of the exfoliated 10 \AA -thick silicate layers improves the strength of elastomeric polymer matrix. More recent work has also shown that clay nanolayers reinforce glassy epoxy matrices under compressive strain (Figure

2.7). The dimensional stability, thermal stability and solvent resistance of the glassy matrix can also be improved when the clay nanolayers are present (Massam and Pinnavaia, 1998).

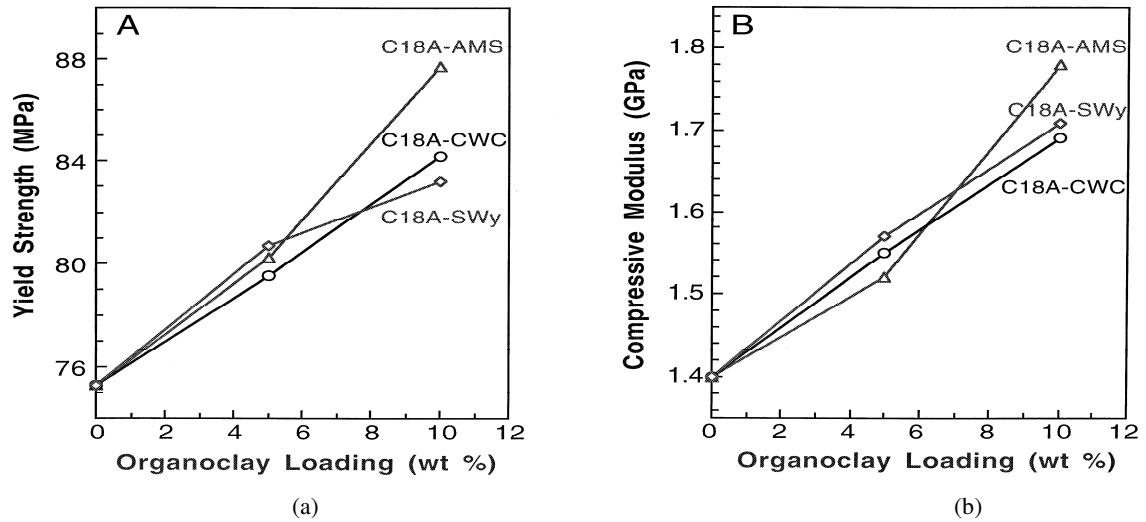


Figure 2.7. a) Compressive yield strength and b) moduli for the pristine epoxy polymer and the exfoliated epoxy–clay nanocomposites prepared from three different kinds of organoclays (Source: Massam and Pinnavaia, 1998).

2.6.2. Layered Silicate/Polyurethane Nanocomposites

The intercalation and exfoliation chemistry of epoxy–clay nanocomposites have been successfully transferred to a thermoset polyurethane system. The maximum benefit from nanolayer dispersal and reinforcement was demonstrated recently by Wang and Pinnavaia, 1998. Solvation of the organoclays by polyols afforded intercalates with basal spacings that were dependent on the chain length of the gallery onium ion, but independent of the molecular weight of the polyol or the cation exchange capacity of the clay. In situ polymerization of polyol–isocyanate precursor–organoclay mixtures afforded nanocomposites containing an intercalated clay phase ; 50 Å basal spacings embedded in the cross-linked polyurethane network. A unique stress–strain behavior was observed for the elastomeric nanocomposites (Figure 2.8). Nanocomposite formation both strengthens and toughens the elastomeric matrix relative to the pristine polymer.

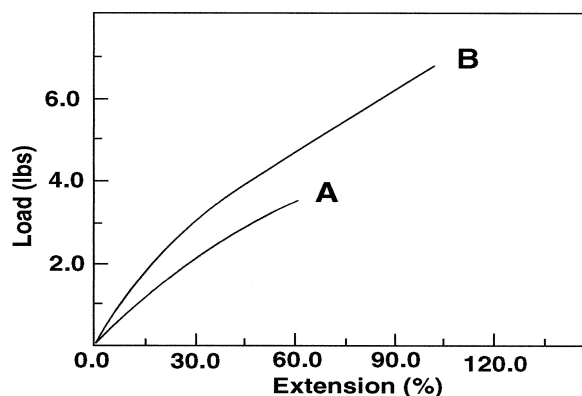


Figure 2.8. Stress–strain curves for A a pristine polyurethane elastomer; B a polyurethane–clay nanocomposite prepared from organomontmorillonite 5 wt.% (Wang and Pinnavaia,1998)

2.6.3. Layered Silicate/Vinyl Polymer Nanocomposites

These material systems include the vinyl addition polymers derived from common monomers such as methyl methacrylate (Nam et al. 2001, Tanaka et al. 1963, Mohanty et al. 2003), methyl methacrylate copolymers (Bafna et al. 2003, Usuki et al. 1997), other acrylates (Sinha et al. 2002, Giannelis 1996), acrylic acid (Nam 2001, Leaversuch 2001), acrylonitrile (Mathias et al. 1999, Sinha et al. 2003), styrene (S) (Usuki 1997, Tetto et al. 1999), vinylpyridine (Vaia et al. 1993), acrylamide (Biswas et al. 2001, Brindly et al. 1980), poly(N-isopropylacrylamide) (Aranda et al. 1992) and tetra-fluoro ethylene (Greenland 1963). In addition, selective polymers such as PVA (Usuki et al. 1991, Krishnamoorti et al. 1996), poly(N-vinyl pyrrolidone) (Giannelis 1996, Yano et al. 1993), poly(vinyl pyrrolidinone) (Yano et al. 1997, Fujiwara et al. 1976), poly(vinyl pyridine) (Gilman et al. 1997), poly(ethylene glycol) (Dubois, 2000), poly(ethylene vinyl alcohol) (Vaia et al. 1996), poly(vinylidene fluoride) (Morgan, 2003), poly(p-phenylenevinylene) (Mathias et al. 1999), polybenzoxazole (Bafna et al. 2003), poly(styrene-co-acrylonitrile) (Yano et al. 1993), ethyl vinyl alcohol copolymer (Yano et al. 1991), polystyrene–polyisoprene diblock copolymer (Sinha et al. 2003, Sinha et al. 2002) and others (Sinha et al. 2003) have been used.

2.6.4. Layered Silicate/Polystyrene Nanocomposites

Different techniques have been employed in order to form polystyrene nanocomposites. In one method, a Cu^{++} exchanged hectorite instead of the more common organoclay was used (Porter et al ,1998) The copper cations were expected to catalyze the oxidation of styrene monomers in the clay galleries, but the approach was unsuccessful, most likely due to the inability of styrene to intercalate into the inorganic clay.

An alternative technique involved the direct bonding of styrene to a vinyl functionalized surfactant exchanged into the organoclay via in situ polymerization (Akelah and Moet, 1996) . Still, it needs a gallery expansion invoked by the addition an organic solvent in order for the styrene to intercalate prior to polymerization. Acetonitrile proved to be the most effective solvent as it gave a 24.5 \AA d-spacing indicating intercalation of styrene as compared to 22.2° and 18.1 \AA for acetonitrile–THF and acetonitrile–toluene mixtures, respectively . Following polymerization the XRD peak for the intercalated clay persisted, indicated that little or no exfoliation of the clay occurred.

The most practical and promising technique for polystyrene intercalation was the melt intercalation of the polymer into the interlayer gallery region of the clay. Both long chain primary and quaternary alkylammonium exchanged clays were examined (Vaia et al.; Vaia and Giannelis 1996). The organoclay was mixed with commercially available polystyrene at a temperature above T_g of the polymer via melt processing. The diffusion of the polystyrene polymer into the intragallery region was a slow process, dependent on many factors such as the polymer molecular weight, processing temperature, alkylammonium chain length and the interactions between the polymer, surfactant and silicate. Under optimal processing conditions, about 10 \AA thickness of polymer was inserted into clay gallery with a very limited fraction of disordered silicate layers presented near the edge of crystallites.

2.6.5. Speciality Polymer Nanocomposite Systems

In addition to the above mentioned conventional polymers, several interesting developments occurred in the preparation of nanocomposites of layered silicates with

specialty polymers including the N-heterocyclic polymers like polypyrrole (PPY) (Tetta 1999), poly(N-vinylcarbazole) (PNVC) (Gilman et al. 1997, Dubois 2000), and polyaromatics such as polyaniline (PANI) (Theng 1979, Brindly et al. 1980), poly(p-phenylene vinylene) (Biswas et al. 2001) and related polymers (Greenland 1963). PPY and PANI are known to display electric conductivity (Krishnamoorti et al. 1996), and PNVC is well known for its high thermal stability and characteristic optoelectronic properties (Lagaly 1986). Research has also been initiated with liquid crystalline polymer (LCP)-based nanocomposites (Vaia et al. 1993), hyper branched polymers (Brindly et al. 1980), cyanate ester (Aranda et al. 1982), and aryl-ethanyl-terminated coPoss imide oligomers (Sinha et al. 2003).

2.6.6. Biodegradable Polymer Nanocomposite Systems

Today, tremendous amounts and varieties of plastics, notably polyolefins, polystyrene and poly(vinyl chloride) produced mostly from fossil fuels, are consumed and discarded into the environment, ending up as wastes that do not degrade spontaneously. Their disposal by incineration produces large amounts of carbon dioxide, and contributes to global warming, some even releasing toxic gases. For these reasons, there is an urgent need for the development of green polymeric materials that would not involve the use of toxic or noxious components in their manufacture, and could allow degradation via a natural composting process. Accordingly, polylactide (PLA) is of increasing commercial interest because it is made from renewable resources and readily biodegradable.

The reported biodegradable polymers for the preparation of nanocomposites are PLA (Yano et al. 1997, Strawhecker 2000, Sinha et al. 2003), poly(butylene succinate) (PBS) (Fujiwara et al. 1976, Dubois 2000), PCL (Yano et al. 1993, Yano et al. 1991), polyhydroxy butyrate (Biswas et al. 2001, Aranda et al. 1992).

2.6.7. Polyolefin Nanocomposite Systems

Polyolefins such as polypropylene (PP) (Sinha et al. 2003, Tanaka et al. 1963), polyethylene (PE) (Tanaka et al. 1963, Garces et al. 2000), polyethylene oligomers (Leaversuch 2001), copolymers such as poly(ethylene-covinyl acetate) (EVA)

(Leaversuch 2001), ethylene propylene diene methylene linkage rubber (EPDM) (Strawhecker 2000) and poly(1-butene) (Tanaka et al. 1963) have been used.

Polypropylene is the lightest major thermoplastic, with a density of about $0,90\text{g/cm}^3$. Its high crystallinity imparts the polymer to have high tensile strength, stiffness and toughness. Polypropylene can be produced in either isotactic or atactic form. It has excellent electrical properties and the chemical inertness. Its moisture absorption is typically like a hydrocarbon polymer. However, the polypropylene is less stable than the other polyolefins like PE, EVA and EPDM to heat, light and oxidative attack. So, it is generally stabilized with oxidants and ultraviolet absorbers.

The dispersal of clay nanolayers into the nonpolar polyolefin systems proves to be a challenge since the polarity of organoclay does not match well with such polymers. Initial attempts to create polypropylene–clay hybrids were based on the introduction of a modified polypropylene with polar groups to mediate the polarity between the clay surface and bulk polypropylene (Kurokawa et al. 1996; Usuki et al.,1997).However, an organic solvent has to be used in order to facilitate the formation of a modified polypropylene intercalate. Only a limited degree of clay nanolayer dispersion was observed by this method.

An alternative and more environmentally friendly method was developed later by the Toyota research group (Kawasumi et al.,1997;Kato et al., 1997;Hasegawa et al.1998). The mixture of stearylammonium-exchanged montmorillonite, maleic anhydride modified polypropylene oligomer and homopolypropylene was melt processed to obtain a successfull polypropylene–clay hybrid wherein a larger fraction of the clay nanolayers were found to be exfoliated. The hydrolyzed maleic anhydride polypropylene intercalated into the organoclay, expanding the galleries, and facilitated the incorporation of polypropylene. Interestingly, the density of maleic anhydride groups has a significant effect on the final morphology and properties of the composite. A mixture of roughly 3:1 by mass of maleic anhydride polypropylene oligomer to organoclay was found to be the most effective in forming hybrid composites. The hybrids exhibit improved storage moduli compared to pristine polypropylene in the temperature range from T_g to 90°C . The significance of nanolayer reinforcement in polypropylene is not as great as in nylon 6, probably due to the lower degree of exfoliation and the introduction of a large amount of oligomer.

2.6.7.1. Effect of Compatibilizer on the Properties of Polypropylene Nanocomposites

The preparation of polypropylene nanocomposites depends on the selection of suitable compatibilizer, optimization of the processing conditions and the organic modification of the clay. Yeh Wang et al. reported that PPgMA compatibilizers give rise to similar degree of dispersion beyond the weight ratio of 3 to 1 with the exception of a compatibilizer (maleic anhydride within the MA content ranging 0.5 to 4.0 wt.%) which had the highest MA content and the lowest molecular weight. The thermal instability and high melt index were responsible for ineffective modification by the compatibilizer. Furthermore, PPgMA with low melting point and high melt index was compounded at low equilibrium temperature in order to maintain a certain level of torque. PPgMA with lower molecular weight and higher MA content leads to good clay dispersion in PP/clay composites; it caused the deterioration in both mechanical and thermal properties of PP/PPgMA/clay composites.

During the melt compounding of PPgMA compatibilizers and organoclay, the intercalation capability of the compatibilizer had been well known due to the polarity of MA in the structure. Besides this, the molecular weight determined the shear viscosity of the compatibilizer played an important role in the breaking up of clay platelets. Therefore PPgMA with the low melting point and high melt strength compounded at low equilibrium temperature helped the intercalation of the molecules into the clay galleries.

Complete hybrid nanocomposites were produced with the PPgMA/clay ratio over 3:1 when compounding in the twin screw extruder. The addition of lower molecular weight PPgMA or high loading of PPgMA had negative effect on the mechanical and thermal properties of PP/PPgMA/clay systems.

Jong Hyun Kim et al., 2004 prepared polypropylene/- layered silicate nanocomposites using an antioxidant and investigated the effects of antioxidant in PP/layered silicate nanocomposites on the mechanical properties and the rheological properties. The tensile modulus of the nanocomposite increases as the clay content increases. The nanocomposite with 3 wt% of silicates has a modulus of 1.33 times higher than the unfilled PP. The significant increase in tensile modulus even at small clay content comes from the nano-scale dispersion of clay in polymer matrix. In general, the deformation behavior of semicrystalline polymers is strongly dependent on the crystallite orientation. The morphology of a nanocomposite directly causes a

remarkable difference in deformation processes, which in turn determines the ultimate macroscopic property (Figure 2.9).

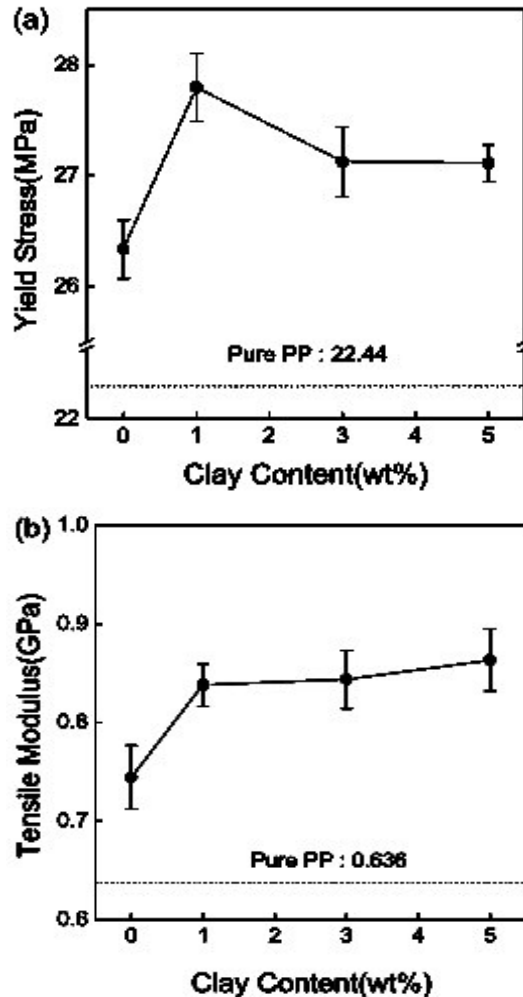


Figure 2.9. Yield stress (a) and Young's modulus (b) of unfilled PP and PPLSNs as a function of organoclay contents at constant loading of antioxidant, 0.5 phr. (Source: Jong Hyun Kim et al., 2004)

Liu et al., 2000 prepared polypropylene/clay nanocomposites via grafting –melt compounding by using co-intercalation organophilic clay that had a larger interlayer spacing than the ordinarily organophilic clay only modified by alkyl ammonium. The mechanical properties of the nanocomposites are improved by clay addition. The incorporation of silicate layers in the PP matrix gives rise to a considerable increase of stiffness and tensile strength. On the other hand, the impact strength is not affected by clay loading.(Figure 2.10-12).

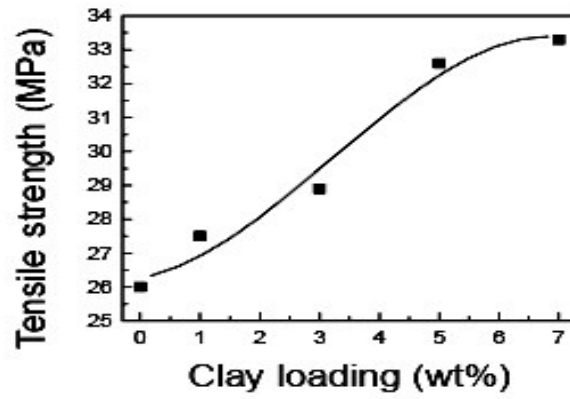


Figure 2.10. Tensile Strength of PP Nanocomposites
(Source:Liu et al., 2000)

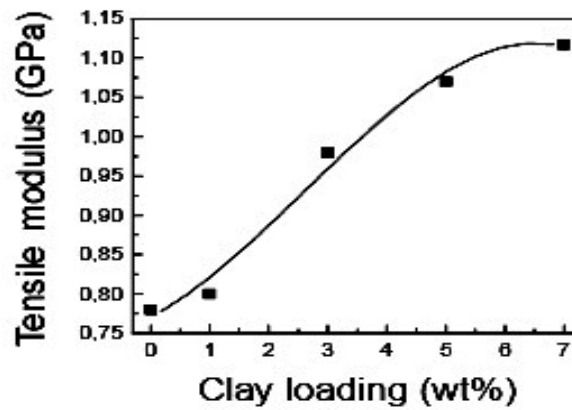


Figure 2.11. Tensile Modulus of PP Nanocomposites
(Source: Liu et al., 2000)

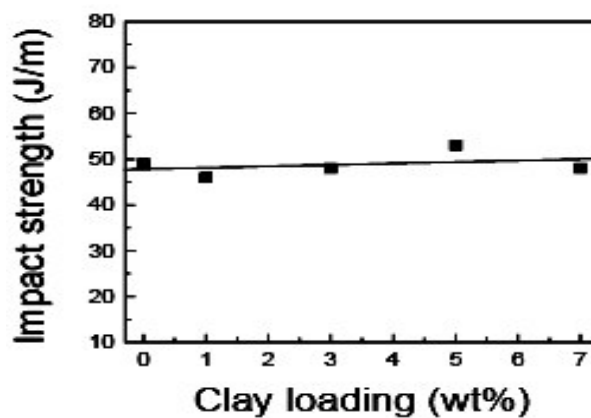


Figure 2.12. Izod Impact Strength of PP Nanocomposites
(Source: Liu et al., 2000)

Hoa et al., (2006) produced polypropylene/clay nanocomposites by melt processing using a Brabender plasticorder. The mechanical results were obtained from dynamic mechanical analysis after six types of nanoclay was blended with polypropylene. All the compositions with nanoclay showed higher storage modulus (stiffness) as compared pure polypropylene all through the temperature range. The nanocomposite structure contains 3wt.% nanoclay, modified by quaternary ammonium compound with a concentration of 120meq/100gr, and showed the highest modulus, almost 20% higher than neat PP at room temperature.

Demin Jia et al. (2005) studied the structure and properties of PP/organo-clay nanocomposites compatibilized with PPgMA by the melt intercalation method. To reveal the effects of the OMMT on the mechanical properties of the PP, the mechanical properties of the matrix (PP/2 wt.% compatibilizer) were compared with those of the neat PP. The flexural modulus of nanocomposites increased remarkably with OMMT content. The flexural modulus of PP/OMMT nanocomposite with 2 wt.% OMMT increased to 2.41 GPa as compared to 1.27 GPa for neat PP (Table 2.1).

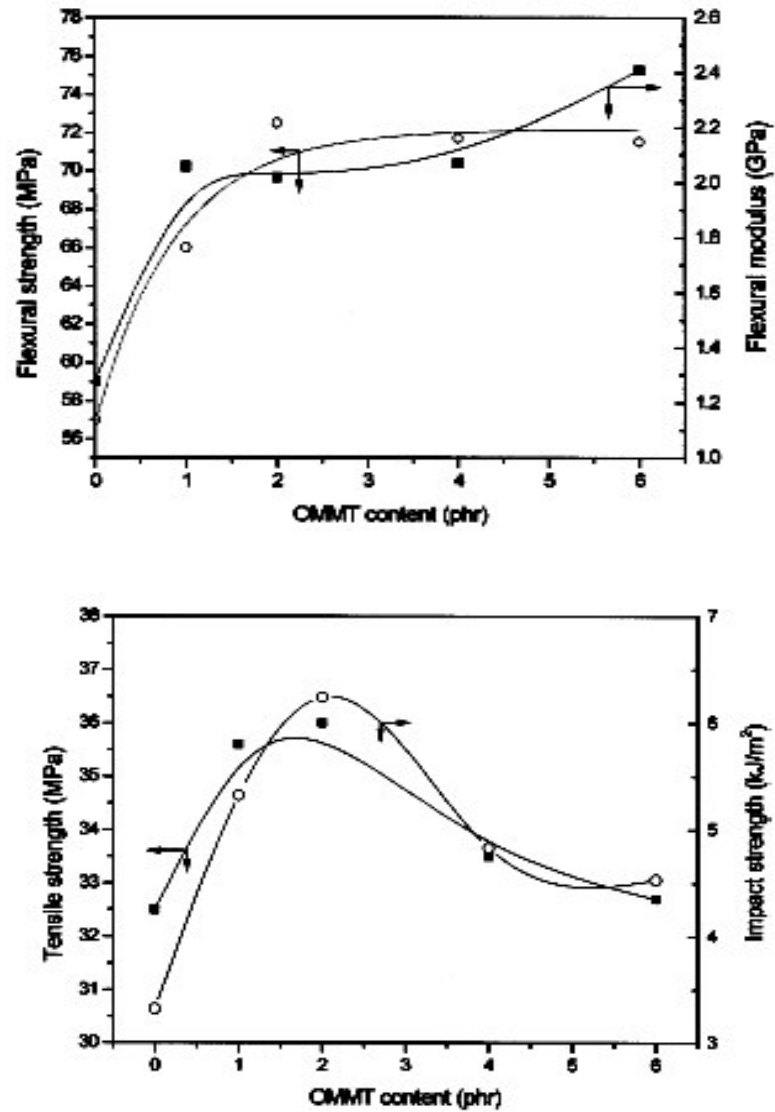


Figure 2.13. Mechanical Properties of PP Nanocomposites
(Source: Demin Jia et al. 2005).

Table 2.1. Mechanical Properties of Compatibilized Nanocomposites
(Source: Demin Jia et al. 2005).

	Tensile Strength(MPa)	FlexuralStrength (MPa)	Flexural Modulus(GPa)	Impact Strength(kJ/m ²)
PP	32.5	57	1.27	3.32
PP/2wt% PPgMA	32.8	59.2	2.41	3.28

The tensile strength, flexural strength and impact strength, however, reached a maximum at an OMMT content of 2 wt.% (Fig 2.13). The significantly increased mechanical properties at low OMMT loading may be due to the uniformly dispersed MMT tactoid with intercalated structures. TMPP promoted the dispersion of OMMT into PP matrix. The fraction of the intercalated structure decreased with the OMMT content. At higher content, aggregation of the OMMT might take place. As a consequence, the mechanical properties of the nanocomposite with higher OMMT content might decrease. Also the compatibilizer with 2 wt.% added OMMT; the impact strength could be improved up to 88% as compared with those for neat PP.

B. Vergnes and W. Lertwimolnun (2005) found that the degree of dispersion was improved by incorporating a maleic anhydride grafted polypropylene (PPgMA). However, this improvement was obtained for concentrations of PPgMA higher than 10 wt%. The clay aggregates became smaller and silicate layers were finely dispersed, as the ratio of PPgMA increased. On the other hand, no further improvement on the dispersibility was observed for PPgMA content above 25 wt%. The effects of processing parameters were also investigated. The state of intercalation, interpreted by interlayer spacing, was globally unaffected by processing parameters. Increasing shear stress, mixing time and decreasing mixing temperature improved clay layer silicate exfoliation. The proportion of exfoliation was characterized by rheological measurements.

Camino et al. (2005) investigated the effect of molecular weight of polypropylene via melt compounding of either homopolymers or heterophasic copolymers in presence of PPgMA as a compatibilizer. The improvement in modulus was larger in homopolymers (28-49%) as compared to heteropolymers (24-33%) in the presence of 3wt.% organoclay with a ratio of clay: PPgMA; was 1:3. The reinforcing effect increased with increasing delamination of the organoclay. This caused an increase in the modulus with increasing melt flow index. The expected increase in elastic modulus, typical of polymer-clay nanocomposites, was shown to be larger when delamination improved. Increase of stiffness did not affect the impact properties even for a 50% increase in modulus.

Elongation at break was strongly reduced in homopolymers as expected in composites, whereas it was unaffected in heterophasic materials or it was even increased when delamination was improved. A lower detrimental effect was also observed when delamination increases in homopolymers. This behavior was to be

attributed to the reinforcing mechanism of flexible clay layers intimately adhering to the polymer chains which increase elastic modulus by hindering chain segmental rotation, but it could follow chain unfolding when the mechanical stress overcomes bonds rotation constraint (Camino et al. ,2005).

Valerio Causin et al. (2005) clarified the influence on polymer–clay nanocomposite systems of such parameters as processing conditions, molecular weight of the polymer, additives, in order to identify the best conditions to obtain nanocomposites characterized by satisfying mechanical properties. An improvement of 51% was observed in flexural modulus of 3wt.% organoclay containing samples by twin screw compounding with PPgMA in the clay:PPgMA ratio of 1:2.5. Also, the yield stress was improved by 24%, but as the temperature was increased in shear processing, the ammonium salts degraded and deteriorated the mechanical values.

M. Modesti et al. (2006) studied of the influence of compatibilizer and processing conditions on the extent and degree of dispersion of the modified nanofillers in PP matrix. The polypropylene-graft maleic anhydride was used as a compatibilizer and contained 1 wt.% of maleic anhydride (MA). Organoclay was added at a ratio of 3.5 and 5 wt.% and PPgMA was kept constant at 6 wt.%. The processing conditions were set at low/high rpm and low/high temperatures. (HH: high rpm, high temperature, HL: high rpm, low temperature , LH: low rpm, high temperature, LL: low rpm, low temperature)

The effects of the processing conditions, clay content as well as compatibilizer on the tensile modulus was illustrated as in Figure 2.14, where the proportional increases of tensile modulus with respect to neat PP were reported. All nanocomposites prepared showed a significant improvement of tensile modulus with respect to unfilled PP. The enhancements were strictly related to the processing conditions, the filler content and the presence of compatibilizer.

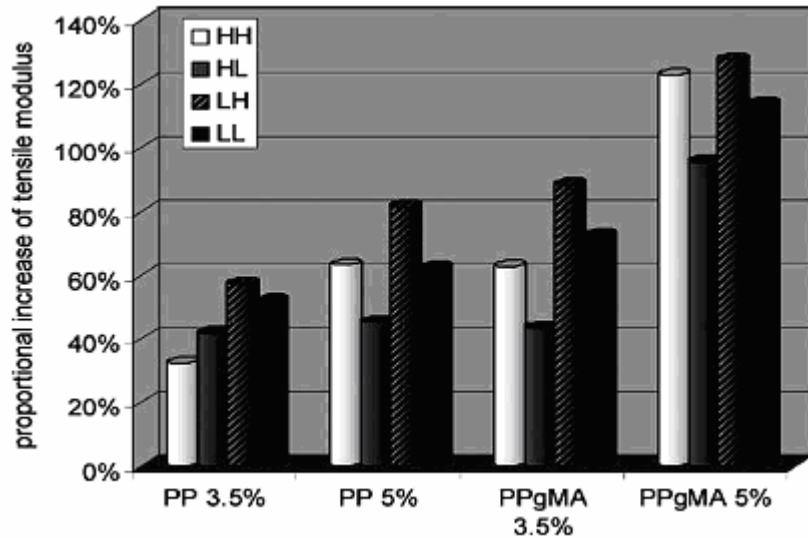


Figure 2.14. Tensile Modulus of PP Nanocomposites

(Source: M. Modesti et al. 2006)

The elastic modulus was higher in the presence of compatibilizer for both filler contents (3.5 and 5 wt. %) owing to the greater interaction between filler and polymer. The results for 5 wt.% filled PPgMA were extremely better: the proportional increase of tensile modulus was found to be about 130%. The yield stress was about 31 MPa and the difference between filled and unfilled materials were lower than 3%. The elongation at yield was about 10.5% for unfilled PP, it decreased to about 9.5% for PP nanocomposites and about 8.5% for PPgMA nanocomposites. The greater interaction was responsible also for the lower elongation at break that was showed for all the specimens tested. In the better case, it dropped from 550% for a neat PP down to 290% for a 3.5 wt.% filled PP, 80% for a 5 wt.% filled PP, 50% for a 3.5 wt% filled PPgMA and 40% for a 5 wt.% filled PPgMA (Figure 2.15).

It was interesting that no nanocomposite structure showed izod value lower than that of unfilled polymer. The increases were higher at higher filler contents; in particular for 5 wt.% PPgMA nanocomposites, processed at lower temperature and higher screw speed (LH), the increase was about 50% with respect to pure PP (Figure 2.16). The enhancement of izod was due to the fact that the exfoliated or intercalated clay layers in nanocomposite play a role in hindering the crack path caused by impact.

These different observations showed that PPgMA nanocomposites combine high stiffness and good ductility at least up to a clay loading of 5 wt.%. Moreover, the

mechanical characterization showed that greater enhancements could be obtained processing the material at the lower barrel temperature profile and higher screw speed. Using PPgMA nanocomposites, processed at suitable conditions, a material that combines high stiffness and good ductility can be obtained.

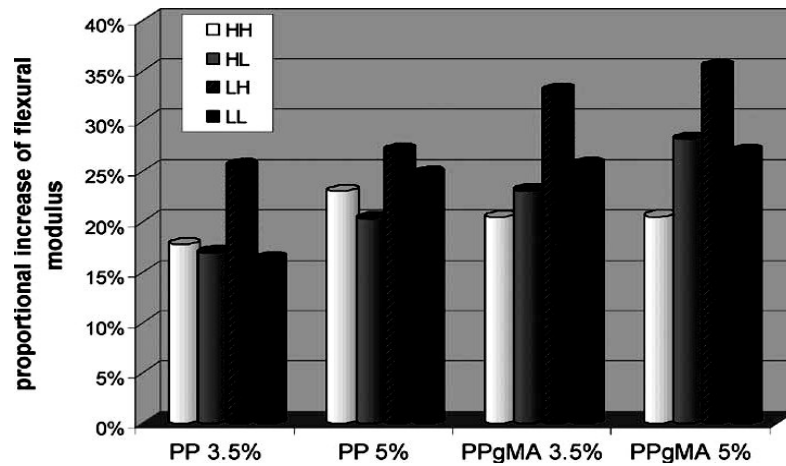


Figure 2.15. Flexural Modulus of PP Nanocomposites
(Source: M. Modesti et al. 2006)

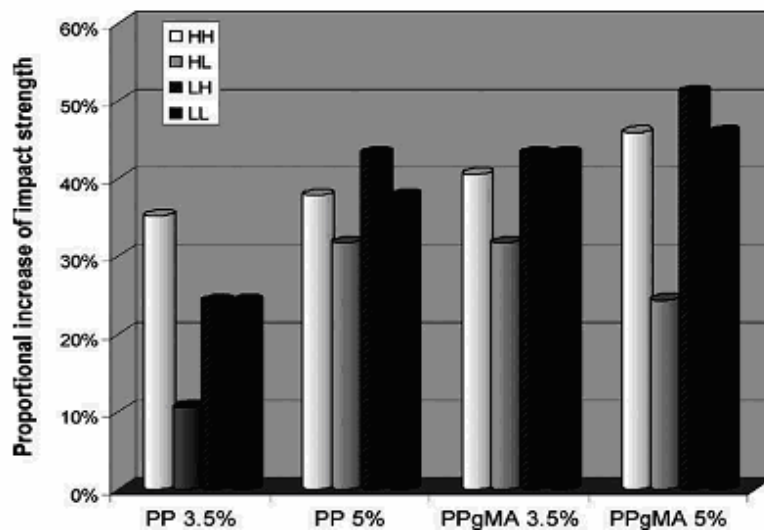


Figure 2.16. Impact Strength of PP Nanocomposites
(Source: M. Modesti et al. 2006)

J.M. Pastor et al. (2003) worked on two different polar coupling agents. Diethyl maleate grafted polypropylene (PPgDEM) and commercial maleic anhydride grafted polypropylene (PPgMA) have been used. The choice of diethyl maleate (DEM) as compatibilizing agent was made because of its high thermal stability, high boiling point and good compatibilization with polyolefins as compared with other compatibilizing agents. Furthermore, the low homopolymerization behavior of DEM, allows a better control of the fictionalization reaction. Maleic anhydride (MAH-1.2wt.%) has been widely used as compatibilizing agent for this kind of systems and it was used as reference on this work. The PP-clay nanocomposites were prepared by melt compounding with two different clays, commercial modified montmorillonite, and sodium bentonite clay.

Tables 2.2 and 2.3 show clay content and mechanical properties of the composites obtained, specifically Young's modulus, tensile strength and notched Izod impact strength. The analysis of the trends on mechanical properties gives information about the effect of both compatibilizing agent and clay. MA is more polar than DEM. DEM has an open structure in which the dipole moment can be close to zero due to transoid conformations. MA is a rigid five member ring with permanent dipole moment. Due to this effect, MA is a better compatibilizing agent, because the polar interactions with the polar clay are more favorable as compared with DEM. Another feature which may explain the improved properties of MA nanocomposites versus DEM is the imide bond formation (J.M. Pastor et al. ,2003).

Table 2.2. Mechanical Properties of DEM Compatibilized PP/Clay Nanocomposites
(Source: J.M. Pastor et al. ,2003).

PP(wt%)	PPgDEM (wt)	Type of Clay	Clay (wt%)	Clay Content(wt%)	Modulus (MPa)	Tensile Strength (MPa)	Notched Izod Impact Strength(kJ/m ²)
100	-	-	-	-	1828±33	34.3±0.9	3.3±0.3
91	9	-	-	-	1799±24	35.2±0.2	2.5±0.4
79	21	-	-	-	1658±39	34.8±0.1	2.8±0.3
88	9	Clay	3	2.0	1780±54	34.7±0.4	3.2±0.4
72	21	Clay	7	5.0	1869±49	33.2±0.3	3.4±0.3
88	9	Organoclay	3	2.1	1902±43	35.0±0.6	2.8±0.3
72	21	Organoclay	7	5.7	2065±22	34.1±0.5	2.6±0.2

Table 2.3. Mechanical Properties of MA Compatibilized PP/Clay Nanocomposites

(Source: J.M. Pastor et.al ,2003).

PP(wt%)	PPgMA (wt)	Type of Clay	Clay (wt%)	Clay Content(wt%)	Modulus (MPa)	Tensile Strength (MPa)	Notched Izod Impact Strength(kJ/m2)
100	-	-	-	-	1828±33	34.3±0.9	3.3±0.3
91	9	-	-	-	1797±81	36.0±0.4	2.4±0.1
79	21	-	-	-	1672±36	35.4±0.2	2.4±0.2
88	9	Clay	3	2.6	2024±43	36.8±0.2	2.2±0.2
72	21	Clay	7	4.8	2130±56	35.5±0.3	1.9±0.4
88	9	Organoclay	3	2.4	2282±27	36.8±0.4	2.5±0.3
72	21	Organoclay	7	4.5	2597±34	36.2±0.1	1.2±0.2

Clay dispersion and interfacial adhesion are greatly affected by the kind of matrix modification. Clay modification and processing conditions are not enough to provide an appropriate nanometric dispersion of clay layers and a homogeneous distribution of the clay in the samples. This might be due to several issues related with thermodynamic interactions in the modified clay–matrix–oligomer system.

The reactivity of MA towards the modifying agent is greater than in the case of DEM. Both factors give a result better of interfacial adhesion and subsequent mechanical performance for MA nanocomposites. Clay and matrix modification are synergistic factors which need to be properly modulated in order to obtain the desired final properties on this kind of non-polar polymer based nanocomposites.

Wilkie et al. (2006) prepared polypropylene and polyethylene nanocomposites from oligomerically modified clay in a Brabender mixer. They found out a decrease in all mechanical properties; tensile strength, modulus and elongation at break values when the lauryl clay was introduced into the system. The mechanical properties were much more affected when the clay loading was increased above the concentration of 4wt.%.

Lee et al. (2004) prepared polypropylene nanocomposites via twin screw extrusion. Their study was mainly focused on the effect of molecular weight of PPgMA on clay dispersion and the mechanical properties of polypropylene nanocomposites. The best mechanical values were found when the PPgMA compatibilizer had the highest molecular weight. The addition of clay to PP always improved the tensile strength and tensile modulus, but reduced its ultimate elongation, regardless of the molecular weight of PPgMA. The most significant increase in tensile strength occurred with the addition of 1 to 2 wt.% of clay. Further addition of clay mainly improved the tensile modulus. Tensile strength and impact strength were affected by the molecular weight of PPgMA.

Ellis et.al (2004) produced polypropylene (PP) nanocomposites containing approximately 4.wt % of an organophilic montmorillonite clay, and characterized its properties with those of talc-filled (20–40 wt %) compositions. Weight reduction, with maintained or even improved flexural and tensile moduli, especially at temperatures up to 70°C, was a major driving force behind the study. The PP nanocomposites exhibited a weight reduction of approximately 12% in comparison with the 20% talc-filled PP, while maintaining comparable stiffness.

2.6.7.2. Thermal Properties of Polypropylene Nanocomposites

Yu-Qing Zhang et al. (2004) in another study, attempted to use grafting-intercalating in situ to synthesize nanocomposites with low compatibilizer content. Polypropylene, an organoclay treated with maleic anhydride (MA), a distending agent, and an initiator were blended together in melt. The graft reaction and high shearing forces simultaneously led to good dispersion of the silicate layer in the grafted polypropylene matrix. The composites resulting from grafting-intercalating, in situ, were used as a master batch and blended with PP to give the final nanocomposites. The thermal properties and dynamic behavior of the nanocomposites were measured to characterize the composites. The OMMT content of the composites was about 30 %.(OMMT/PPgMA was 1:3).The organoclay content varied from 1 to 4wt. %.

The introduction of lower-molecular weight PPgMA into the PP matrix decreased the Tg of the material due to plasticization. By contrast, the Tg of PP/clay nanocomposites did not decrease, but increased with the addition of PPgMA. The Tg of nanocomposites with 4 wt.% clay content was 30 oC higher than those for PP.

With increasing clay content, the melting point of the composite decreased slightly, as compared to pure PP. The melting temperature of nanocomposites was thought to decrease due to the effects of the PPgMA on the crystal integrity of PP, but this interference was very weak. However, the introduction of clay into PP enhanced the thermal stability of PP greatly. Comparing the thermal decomposition temperature of PP nanocomposites with that of pure PP, the temperature at the onset of the thermal decomposition of PP nanocomposites with 2 wt.% clay content was increased by nearly 130 °C.

The weight loss curve of the nanocomposites with 2 wt.% clay content was nearly a vertical line, which means that the decomposition was very fast. The enhanced thermal stability of the polymer–clay nanocomposites was attributed to the lower permeability of oxygen and the diffusibility of the degradation products from the bulk of the polymer caused by the exfoliated clay in the composites (Lagaly, 1986, Usuki et.al 1997, Dubois, 2000).

The conclusion was that the introduction of clay into the PP matrix improved the thermal stability of the PP remarkably. The narrow space surrounded by the dispersed clay layers and the interaction between the clay layers and macromolecules restricted the motion or relaxation of the chain segment of the PP, which was increasing T_g.

Demin Jia et.al (2005) found that the WAXS patterns of PP and PP/OMMT nanocomposites showed that the addition of OMMT did not affect the crystal structure of the PP matrix. The addition of PPgMA had minimal effects on the crystallization behavior of PP, the crystallization peak temperature of PP/OMMT nanocomposite with 1 wt.% OMMT increased to 125.4 oC as compared with 114.4 oC for neat PP. The DSC results clearly showed that the addition of a small amount of OMMT into the PP matrix resulted in an increase of crystallization temperature. This phenomenon might be due to the efficient nucleating effects of the silicate layers/ tactoids.

The TGA analysis for neat PP, PP/2 wt% PPgMA and PP/OMMT stated that PPgMA could improve the stability at high temperature while it showed adverse effect on the stability at lower temperature. All PP/OMMT nanocomposites showed overall higher thermal stability as compared with neat PP. The initial thermal stability was characterized by the temperatures at 5 and 10% weight loss.

The PP/OMMT nanocomposites showed substantially improved initial thermal stability as compared with neat PP. At relatively lower OMMT content, the initial thermal stability increased with OMMT content. The PP/OMMT nanocomposite with 4wt.% OMMT showed the highest initial thermal stability.

Demin Jia et al. (2005) concluded that the incorporation of silicate layers and PPgMA gave rise to a considerable increase in impact strength and flexural modulus as compared with the neat PP. The crystallization peak temperature of nanocomposites was about 10 oC higher than that of PP. By adding 4wt. % OMMT, the temperature at 5 wt.% weight loss of the nanocomposite was 38 oC higher than that of neat PP. The T_g of PP was lowered by the incorporation of the OMMT. The changes of the properties could be correlated with the formation of the PP/OMMT nanocomposites.

Bertini et.al (2006) produced polypropylene (PP) montmorillonite nanocomposites using isotactic PP homopolymers with different rheological properties, and a maleic anhydride grafted PP. Their study concluded the efficiency of the silicate layers in delaying the polymer decomposition during thermal oxidation.

The weight loss was slowed down in all the composites with a larger effect in maleic anhydride grafted PP. The different increase in thermal stability registered for the nanocomposites was likely related to the different degree of exfoliation. The improvement in the thermal stability was probably due to a physical barrier effect of the silicate layers. The barrier effect concerned the diffusion of the volatile thermal oxidation products to the gas phase and, at the same time, of the oxygen from the gas phase to the polymer matrix.

Modesti et.al (2006) investigated the thermal properties and fire behaviour of polypropylene (PP) nanocomposites using differential scanning calorimetry. The nanocomposites were prepared using the melt intercalation technique containing 3.5 and 5wt.% nanoclay, in a co-rotating intermeshing twin screw extruder. The influence of different processing conditions (barrel temperature profile and screw rate) and compositions of PP and nanoclay blends (clay content, use of compatibiliser) on the thermal properties of the nanocomposites were examined.

The results showed that all the properties analysed were strongly influenced by the nanocomposite composition; instead, the processing conditions greatly affected only the dynamic-mechanical properties. DSC curves showed that the crystallinity was deeply influenced by the presence of the clay in the matrix, owing to the fact that the filler acts as nucleating agent.

TGA traces in oxidizing atmosphere showed a drastic shift of the weight loss curve towards higher temperature and no variation of the onset temperature (i.e. the temperature at which degradation begins). The TGA analyses in inert atmosphere showed instead marked increase of this parameter (about 200 oC) and no shift of weight loss curves.

Camino et.al (2005) investigated the effect of molecular weight of polypropylene via melt compounding of either homopolymers or heterophasic copolymers in the presence of PPgMA as a compatibilizer on the thermal decomposition behavior.

The presence of organoclay modified the thermal oxidative volatilization behaviour of the polymer in all the composites, increasing the temperature at which

volatilisation occurs, due to a barrier labyrinth effect slowing down the diffusion rate of degradation products from the bulk of the polymer to the gas phase and also of oxygen from the gas phase into the polymer matrix. Volatilisation of the polymer led to reassembling of the clay layers into the phyllosilicate structure, which created a skin that maximized the protective barrier effect towards the underlying material.

The fact that a similar behaviour was found for all the nanocomposites independent of their morphology indicates that effectiveness of the ablative reassembling process in providing the high temperature protective skin was apparently not affected by the type of clay delaminated morphology whether exfoliated or intercalated when heating occurs in dynamic conditions.

Lei et.al (2006) studied the effects of clay on polymorphism of polypropylene (PP) in PP/clay nanocomposites. He reported an increase in the crystallization temperatures due to the nucleation effect of organoclay. In the same study, the melting temperatures of the PPCN's were decreased when compared with the neat PP. This can be a result of introducing low molecular weight surface modifier used in organoclay synthesis.

Sarazin et.al (2005) produced polypropylene nanocomposites by melt blending using different clays and coupling agents based on maleic anhydride-grafted PP. The use of low molecular weight PPgMA led to a good and uniform intercalation, but with no further possibility to exfoliation. The higher molecular weight of PPgMA supplied a heterogeneous intercalation with exfoliation. 2wt.% clay loading with the use of 4wt.% compatibilizer, significantly affected the crystallization of PP. The presence of the low molecular weight PPgMA caused the crystallization of PP occur at higher temperatures at higher rates with the organoclay. The results were in agreement with the importance of the spherulite size reduction.

2.6.8. Other Properties of Nanocomposites

2.6.8.1. Gas barrier properties

Clays are believed to increase the barrier properties by creating a maze or "tortuous path" (Figure 2.17) that retards the progress of the gas molecules through the matrix resin. The direct benefit of the formation of such a path was clearly observed in

polyimide/clay nanocomposites by dramatically improved barrier properties, with a simultaneous decrease in the thermal expansion coefficient (Yano et al. 1991, 1993, 1997). The polyimide/layered silicate nanocomposites with a small fraction of organo-modified layered silicates exhibited reduction in the permeability of small gases, e.g. O₂, H₂O, He, CO₂, and ethyl acetate vapors (Giannelis, 1996). For example, at 2 wt.% clay loading, the permeability coefficient of water vapor was decreased ten-fold with synthetic mica relative to pristine polyimide. By comparing nanocomposites made with layered silicates of various aspect ratios, the permeability was seen to decrease with increasing aspect ratio.

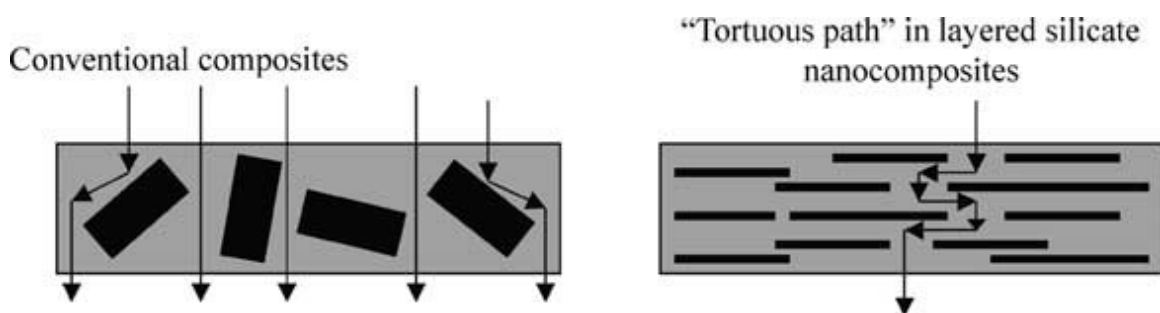


Figure 2.17. Formation of tortuous path in polymer layered silicate nanocomposites.

(Source: Giannelis, 1996)

2.6.8.2. Fire retardant properties

The cone calorimeter is one of the most effective bench-scale methods for studying the fire retardant properties of polymeric materials. Fire-relevant properties such as the heat release rate (HRR), heat peak HRR, smoke production, and CO₂ yield, are vital to the evaluation of the fire safety of materials. In 1976, Unitika Ltd, first presented the potential flame retardant properties of PA6/layered silicate nanocomposites (Fujiwara et al. 1976). Then in 1997 Gilman et al. reported detailed investigations on flame retardant properties of PA6/layered silicate nanocomposite.

Lei et al. (2003) investigated the flammability character of polypropylene in the presence of PPgMA, organoclay and PA6. The cone calorimeter analysis showed that the heat release rate of flame retarded PP was reduced by an amount of 77% in the presence of 8wt.% PPgMA and 5 wt.% organoclay.

2.6.8.3. Optical Transparency

Although layered silicates are microns in lateral size, they are just 1 nm thick. Thus, when single layers are dispersed in a polymer matrix, the resulting nanocomposite is optically clear in visible light. Figure 2.18 presents the UV/visible transmission spectra of pure PVA and PVA/Na⁺-MMT nanocomposites with 4 and 10 wt% MMT. The spectra show that the visible region is not affected by the presence of the silicate layers, and retains the high transparency of PVA. For UV wavelengths, there is strong scattering and/or absorption, resulting in very low transmission of UV light. This behavior is not surprising, as the typical MMT lateral sizes are 50–1000 nm. Like PVA, various other polymers also show optical transparency after nanocomposite preparation with organo-modified MMT (Fujiwara et al. 1976, Gilman et al. 1997).

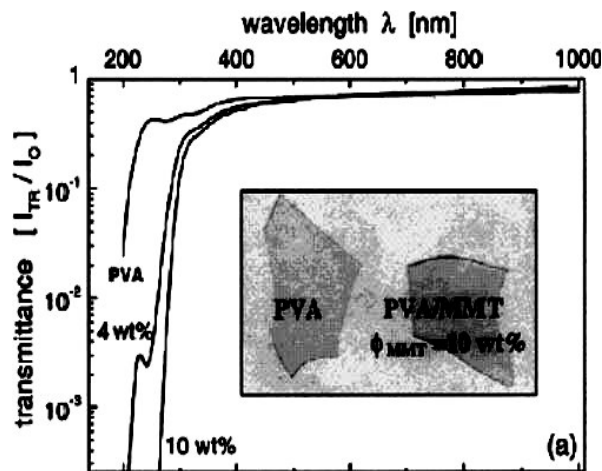


Figure 2.18. UV transmittance spectra of PVA and PVA/MMT nanocomposites 4 and 10 wt% MMT (Source: Dubois, 2000).

2.6.8.4. Biodegradability

Another interesting and exciting aspect of nanocomposite technology is the significant improvement of biodegradability after nanocomposite preparation with organo-modified MMT. Tetto et al., 1999 first reported results on the biodegradability of nanocomposites based on polycaprolactam (PCL), reporting that the PCL/OMLS nanocomposites showed improved biodegradability as compared to pure PCL. The improved biodegradability of PCL

after nanocomposites formation may be due to a catalytic role of the organo-modified MMT in the biodegradation mechanism, but this was not clear. Recently, Lee et al., 2002 reported the biodegradation of aliphatic polyester (APES)-based nanocomposites. Figure 2.19 shows the clay content dependence of the biodegradation of APES-based nanocomposites prepared with two different types of nanoclays.

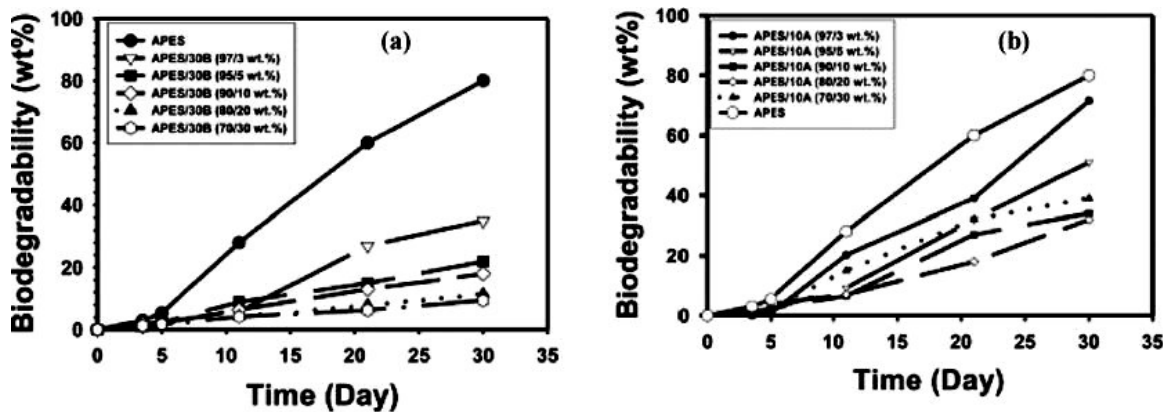


Figure 2.19. Biodegradability of APES nanocomposites with: (a) Cloisite 30B and (b) Cloisite 10A (Source: Lee et al. 2002).

They assumed that the retardation of biodegradation was due to the improvement of the barrier properties of the aliphatic APES after nanocomposite preparation with clay.

Very recently, Sinha Ray et al. (2002, 2003) reported the biodegradability of neat PLA and the corresponding nanocomposites prepared with octadecyltrimethylammonium- modified MMT (C18C3-MMT), along with a detailed mechanism of the degradation. The samples used was prepared from food waste, and tests were carried out at a temperature of $(58 \pm 2)^{\circ}$ C. Figure 2.14a shows the recovered samples of neat PLA and PLACN4 (4 wt.% organo-modified MMT containing). The decrease in M_w and residual weight percentage of the initial test samples were also reported as illustrated in Figure 2.14b.

Obviously, the biodegradability of neat PLA was significantly enhanced after nanocomposite preparation with organo-modified MMT. Within one month, both the extent of M_w and the extent of weight loss were at the same level for both neat PLA and PLACN4. However, after one month, a sharp change occurred in the weight loss of PLACN4, and within 2 months it was completely degraded by compost.

The presence of terminal hydroxylated edge groups in the silicate layers may be one of the factors responsible for this behavior. In the case of PLACN4, the stacked (4 layers) and intercalated silicate layers are homogeneously dispersed in the PLA matrix (from TEM image), and these hydroxy groups start heterogeneous hydrolysis of the PLA matrix after absorbing water from the compost. This process takes some time to start. For this reason, the weight loss and degree of hydrolysis for PLA and PLACN4 are almost the same up to 1 month (Figure 2.20-21).

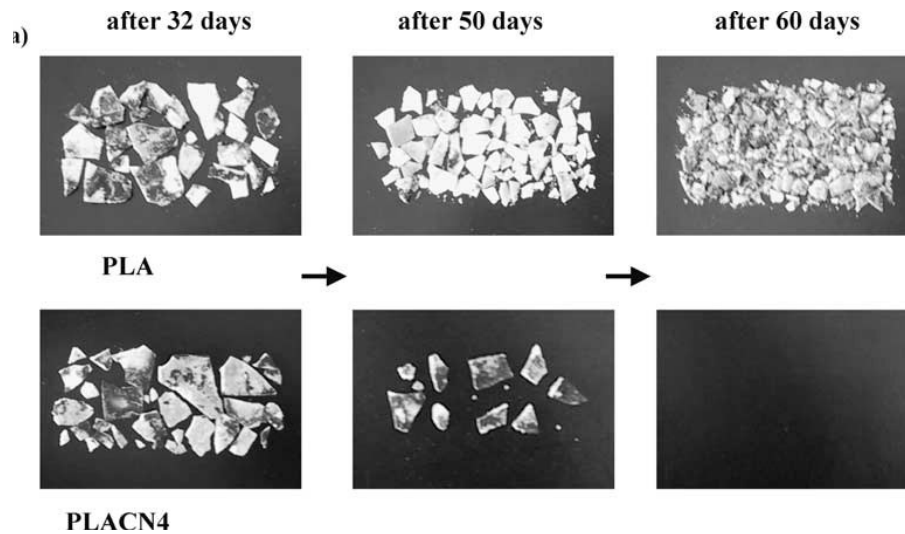


Figure 2.20. Real picture of biodegradability of neat PLA and PLACN4 with time.
(Source: Sinha et.al 2002)

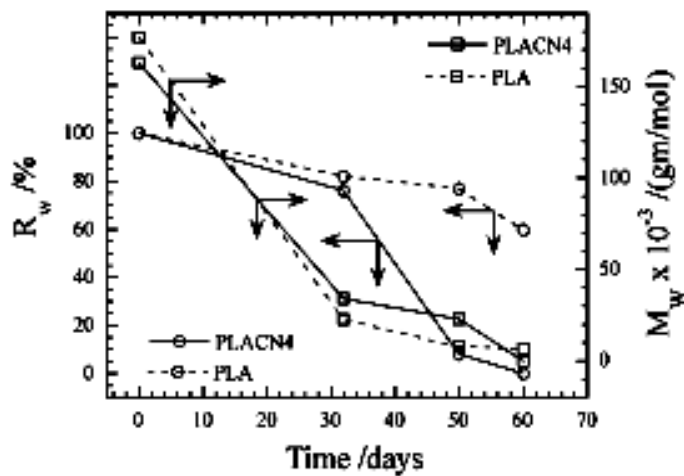


Figure 2.21. Time dependence of residual weight, R_w and M_w of PLA and PLACN4 at $58 \pm 2^\circ\text{C}$ (Source: Sinha et.al 2003)

However, after 1 month there was a sharp weight loss in the case of PLACN4 as compared to that of PLA. That means that 1 month is the critical timescale to start heterogeneous hydrolysis, and due to this type of hydrolysis, the matrix decomposes into very small fragments and eventually disappears with the compost. This assumption was confirmed by conducting the same experimental procedure with PLACN prepared with dimethyldioctdecylammonium salt modified synthetic mica, which has no terminal hydroxylated edge group. The same degradation tendency was found with PLA (Sinha et.al 2002).

A respirometric test was also used to study the degradation of the PLA matrix in an environment at $(58 \pm 2)^\circ \text{C}$ (Sinha et.al 2002). For this test the environment was made from bean-curd refuse, food waste, and cattle feces. Unlike the weight loss, which reflected the structural changes in the test sample, CO_2 evolution provides an indicator of the ultimate biodegradability of PLA in PLACN4 (prepared with (N(coco alkyl)N,N-(bis(2-hydroxyethyl))-N-methylammonium modified synthetic mica), via mineralization, of the samples. The presence of clay may cause a different mode of attack on the PLA component due to the presence of hydroxy groups.

2.7. Modeling of Nanocomposites

Mechanical behaviour and elastic modulus prediction is important in the development of nanocomposites. The information obtained from these predictions can be a reference in polymer nanocomposites synthesis in order to adjust some mechanical properties such as tensile modulus. The main purpose of a number of theories is to foresee the predictive behavior of the models on the mechanical property of the composite material by considering the properties of constituents (matrix and filler); i.e. Poisson's ratio, modulus, volume fraction, filler aspect ratio, filler distribution, etc. In order to obtain tractable solutions, the theoretical approach has two major assumptions (Whitney and McCullough, 1990):

- The phase surfaces are assumed to be in direct contact and bonded, so that slip does not occur at the interface of the phases.
- The overall average response of the materials to loads is considered rather than localized variations in the material response characteristics.

The theory of rigid particles in a non-rigid matrix was earlier developed by Einstein (Einstein, 1956) for the viscosity of the suspension of rigid spherical particles in compliant matrix. This model was further developed by Mooney (Mooney, 1951), Brodnyan (Brodnyan, 1959) and Guth (Guth, 1945).

The Hashin and Shtrikman modification considered the Poisson contraction of the constituent phases (Hashin and Shtrikman, 1963). The simplest case for a two phase system includes series and parallel models given by Broutman and Krock (Broutman and Krock, 1967). A simpler model for two phase system was proposed by Counto, assuming perfect bonding between the matrix and particle (Counto, 1964).

The two-phase model suggested by Takayanagi has been widely used to predict the modulus of polymers, polymer blends, and composites (Takayanagi et al., 1964). Halpin, who modelled laminated system of randomly oriented fibers or an oriented distribution of fibers in the bulk matrix (Halpin, 1969), studied the stiffness of short fiber reinforced composites with variable fiber aspect ratios. Lewis and Nielsen worked on dynamic mechanical properties of particulate-filled composites and found that the moduli of composites increase with decreased particle size (Lewis and Nielsen, 1970). Chantler et al. (Chantler et al., 1999) present a new phenomenological model based on the classic Hertzian elastic contact theory. Their expressions are generally based on some physical arguments and determination of fitting parameters (Lingois and Berglund, 2002).

For conventional composites containing inorganic fillers, dispersed particle is in the range of micrometers, and the interfacial region is often neglected. Therefore, the interfacial contribution is neglected. When the dispersed particle gets very smaller in size, the specific surface area becomes very large that causes the areal fraction of the interfacial region to be so large.

Some semi-empirical models that rely on the determination of adjustable parameters have been developed due to the complexity of the geometrical features (filler aspect ratio, volume fraction, filler orientation, etc.) and inadequacies of the theoretical models as mentioned above. All of the theoretical modelling approaches based on the relations of the elastic constants given in Equation 2.1. For isotropic materials, there are three elastic constants; the Young's modulus (E), the shear modulus (G), and the Poisson's ratio (ν) to define the the elastic response of the composites.

$$G = \frac{E}{2(1 + \nu)} \quad (2.1a)$$

$$E = \frac{9KG}{3K + G}, \quad \nu = \frac{3K - 2G}{2(3K + G)} \quad (2.1b,c)$$

where K refers to the bulk modulus of the material.

2.7.1. Semi Empirical Predictions for Non-spherical Particulate Systems

The clay platelets are in the forms of layered stacks, models confiding non-spherical particles are more appropriate. There are several important models which have prediction capability of elastic modulus of the non-spherical filled composite systems. Three of them are considered for the estimation of elastic modulus of inorganic layered silicate/thermoplastic polymer nanocomposites.

2.7.1.1. Guth Model

For non-spherical filled particulate composites, this model considers the chains composed of spherical fillers, as rod like filler particles embedded in a continuous matrix. A new expression is developed in the following form:

$$E_c = E_m [1 + 0.67\alpha Vf + 1.62(\alpha Vf)^2] \quad (2.2)$$

where α is the shape factor (length/breadth of the filler), E_m is the elastic modulus of the matrix and E_c is the elastic modulus of the composite. The second term in Equation 2.2 is the contribution of particle-particle interaction that describes the mechanical reinforcement (Flandin et al., 2001).

2.7.1.2. Brodnyan Model

The Mooney (Money,1951) equation is a derivation of the Einstein equation that is in the following form:

$$E_c = E_m \exp\left(\frac{K_E V_f}{(1 - V_f / \phi_m)}\right) \quad (2.3)$$

where ϕ_m is the maximum packing for the given filler, or it is the ratio of true filler volume to the volume the filler actually occupies and K_E is the Einstein coefficient. This relation was modified for non-spherical particles by Brodnyan to incorporate “ α ” the aspect ratio of the particle ($1 < \alpha < 15$). Hence, Equation 2.3 becomes as in the following form (Brown and Ellyin, 2005):

$$E_c = E_m \exp\left(\frac{2.5V_f + 0.407(\alpha - 1)^{1.508}V_f}{(1 - V_f / \phi_m)}\right) \quad (2.4)$$

2.7.1.3. Halpin-Tsai (HT) Method

Halpin-Tsai predictions are generally preferred in order to predict reinforcement effect of fillers in nanocomposite systems with both spherical (or near spherical) and non-spherical filled systems (Fornes and Paul,2003). Halpin-Tsai equations was modified by Wu et al. 2004 for the plate-like filler as in the following form:

$$E_c = \frac{E_m (1 + \xi \eta V_f)}{1 - \eta V_f} \quad (2.5a)$$

where

$$\eta = \frac{E_f / E_m - 1}{E_f / E_m + \xi} \quad (2.5b)$$

Here, E_f refers to the elastic modulus of the filler, and ξ is the shape factor depending on the filler orientation and loading direction. For the rectangular plate-like

filler in a composite system, ξ is equal to $2w/t$, in which w is the width and t is the thickness of the dispersed phase.

Halpin–Tsai equations treat a fiber as a fiber and disk as a rectangular platelet, since the length and, in turn, aspect ratio across a disk is not constant, since length varies across disc-like platelet.

2.7.1.4. Modified Halpin-Tsai Model

Lewis and Nielsen (Lewis and Nielsen 1970, Nielsen 1970) improved the Equation 2.5 and considered the maximum volumetric packing fraction of the filler, ψ , as an additional parameter for increasing the prediction capability of the conventional HT model. Maximum volumetric packing fraction is defined as the ratio of true volume of the filler to apparent volume occupied by the filler. Modified Halpin-Tsai model can be expressed as;

$$E_c = \frac{E_m(1 + \xi \eta V_f)}{1 - \psi \eta V_f} \quad (2.6a)$$

where

$$\psi = 1 + \left(\frac{1 - V_f^{\max}}{(V_f^{\max})^2} \right) V_f \quad (2.6b)$$

CHAPTER 3

EXPERIMENTAL

3.1. Materials

The Na⁺-Montmorillonite (MMT) was used as the source of nanofiller. MMT was supplied from Aldrich (K10) and used as received. For the modification of MMT, hexadecyltrimethylammonium chloride (HTAC, Aldrich) with 25 wt. % solution in water was used with hydrochloric acid.

The polypropylene (MH418), PETKİM Petrochemical, Turkey, an injection grade of homopolymer and maleic anhydride polypropylene, PPgMA, (Fusabond M613-05) as a compatibilizer were used. The properties and the suppliers of the raw materials are given in Table 3.1.

Table 3.1. The properties and suppliers of the raw materials used in the study.

Name	Property	Supplier
PP Homopolymer (MH418)	MFI(at190°C) : 4.0-6.0 gr/10min	PETKİM Petrochemicals, Turkey
PPgMA – Fusabond M613-05	MFI(at190°C) : 120 gr/10min, MA content 0.5%.	DuPont
MMT, Montmorillonite- K10	CEC : 120mequiv./gr, Effective surface area :220gr/m ²	Aldrich
HTAC	25 wt. % solution in water	Aldrich

3.2. Organic Modification of Clay

Clay modification procedure is based on the conventional methods of ion exchange reaction between alkyl ammonium cations and Na⁺-MMT. 20 grams of MMT was dispersed into 400 mL deionized water and stirred at a temperature of 80 °C. 0.05 moles of HTAC was mixed together with 4.8 ml HCl by adding 100 mL deionized water. This solution was poured into the hot clay-water mixture and stirred at a temperature of 80 °C for 1 hour. When a white precipitate formed, the clay slurry was then filtered and

washed with water until no chloride ions were detected. Chloride detection was held by using AgNO_3 as reported in the literature (Salahaddin, 2004). The organoclay (OMMT) was then obtained after drying at 75°C for 2-3 days in a vacuum media.

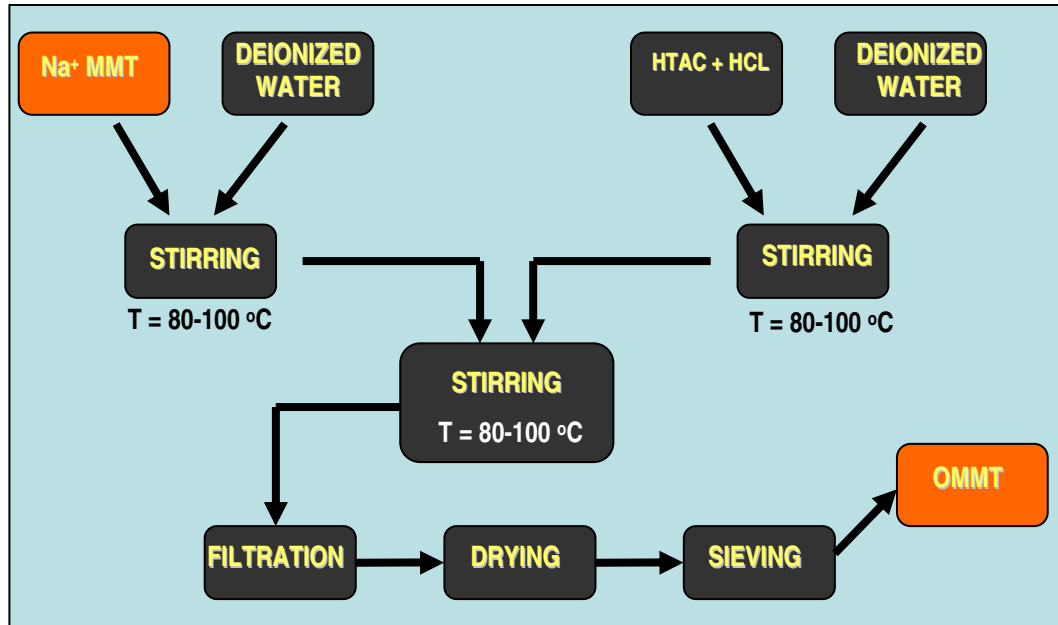


Figure 3.1. Processing Stages of Organic Modification of Clay

3.3. Compatibilization of Organoclay with PPgMA

The compatibilization of organo-modified clay was performed by blending the OMMT particles with PPgMA with weight ratio of 1:3 (organo-modified clay : PPgMA) in a Haake compounding mixer. First, 45 cm^3 PPgMA was melted at 190°C for 1 min. and then clay particles were blended for 10 min. The blend was collected and left for cooling at room temperature. The cooled samples were chopped to further blend them with neat PP.

3.4. Production of Layered Silicate/Polypropylene Nanocomposites

The production of polypropylene nanocomposites is shown in Figure 3.2. The homopolymer PP was fed into Haake two-roll mixer at 190°C (Figure 3.3). After melting of the PP in 1 min, clay particles in the amounts of 3, 5 and 10 wt. % were added into molten PP and the mixing was continued for 10 min in the mixer. The

blended samples were collected and left for cooling. After cooling, the blends were pressed into 100 mm x 100 mm samples having a thickness of 1 mm using a hot press at 190°C (Fig 3.4). The tensile specimens were prepared by a pneumatic cutter and then the samples were left for two days to complete crystallization (Fig 3.5).

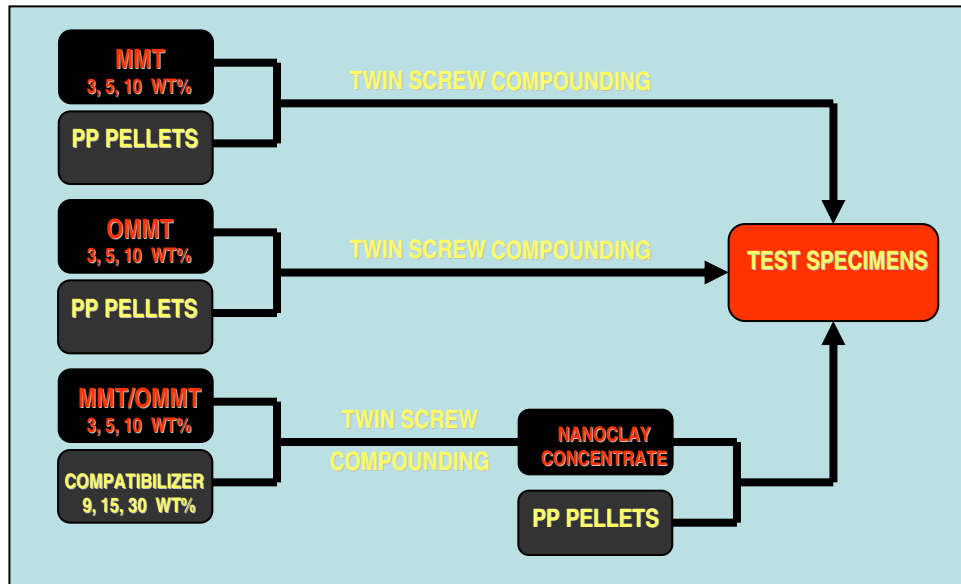


Figure 3.2. Processing Stages for clay/PP Nanocomposites

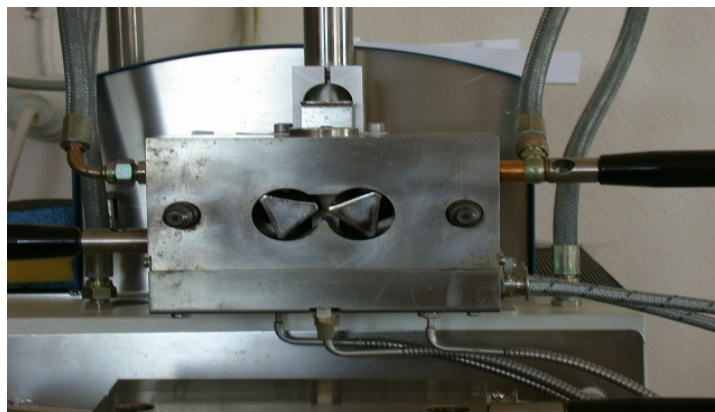


Figure 3.3. Two-roll compounding mixer



Figure 3.4. Hot Press

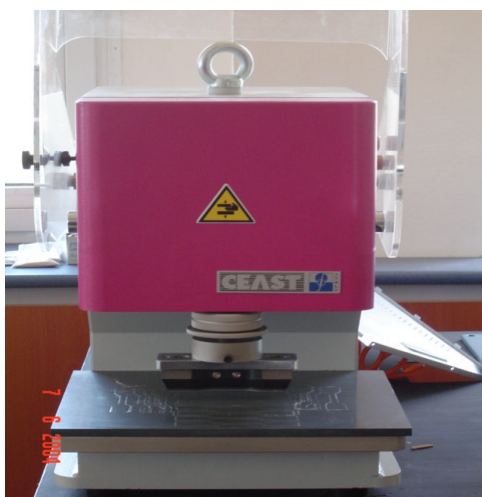


Figure 3.5. Hollow Die Punch and Sample Cutter

3.5. Characterization of Nanocomposites

3.5.1. X-ray Diffraction Analysis

XRD was performed using a PhillipsTM XPert diffractometer with CuK α as a radiation source, operated at 40 kV and 30 mA. The scanning speed was 0.05 deg./min. Powdered specimens were analyzed to determine the characteristic peaks of clay and PP and to determine the basal spacing of silicate layers.

3.5.2. Scanning Electron Microscopy (SEM)

Scanning electron microscopy (SEM) ,PhillipsTM ,was used to investigate the fracture surfaces of the composites.

3.5.3. Tensile Behavior of Nanocomposites

Tension tests were performed on the prepared samples using a Shimadzu AGI 250kN Universal test machine at a crosshead speed of 50 mm/min according to ASTM D638. Tensile modulus, tensile strength and tensile stress at break values were measured.

3.5.4. Thermal Behavior of Nanocomposites

Melting temperature (T_m) and crystallization temperature (T_c) of the samples were measured by differential scanning calorimetry (DSC) under nitrogen flow of 50 mL/min. For this test, samples of 5–6 mg of PP or clay/PP nanocomposites were placed into the aluminium crucibles. Indium was used to calibrate the thermal response due to heat flow as well as the temperature prior to analysis. The dynamic measurements were made at a constant heating rate of 10°C/min from 20 to 220°C, holding the sample at 220 °C for 10 min and then cooling at a rate of 10°C/min to 20 °C to determine the effect of the clay on the T_m and T_c . Further DSC analysis was done to obtain the degradation temperature of clay/PP nanocomposites. For this purpose, the test conditions mentioned above remained the same except the samples were heated up to 600°C, and then cooled to room temperature at a rate of 10°C/min.

3.5.5. Optical Property Characterization

Optical characterizations were done by using HR2000 UV-VIS spectrometer from Ocean Optics. The transmission measurement was done on samples with thickness of 1 mm.

3.5.6. Flammability of Nanocomposites

Flammability of the nanocomposites was evaluated using the UL-94 method according to the ASTM D-635. The UL 94 test determines the material's tendency to extinguish or to spread the flame once the specimen has been ignited. This test method covers a small scale laboratory screening procedure for measuring the relative rate of burning and/or extent and time of burning of self supporting plastics in the form of bars. A specimen is supported in a horizontal position and is tilted at 45° as shown in Figure 3.6. Samples of 125 ± 5 mm in length and 12.5 ± 0.2 mm in width were cut from hot pressed plates. A flame is applied to the end of the specimen that is tilted at 45° to produce a blue flame, and 20 mm high for 30 seconds or until the flame reaches the 25 mm mark. If the specimen continues to burn after the removal of the flame, the time is recorded for the specimen for a specific length during burning. The burning rate is calculated by using the information provided by length and time.

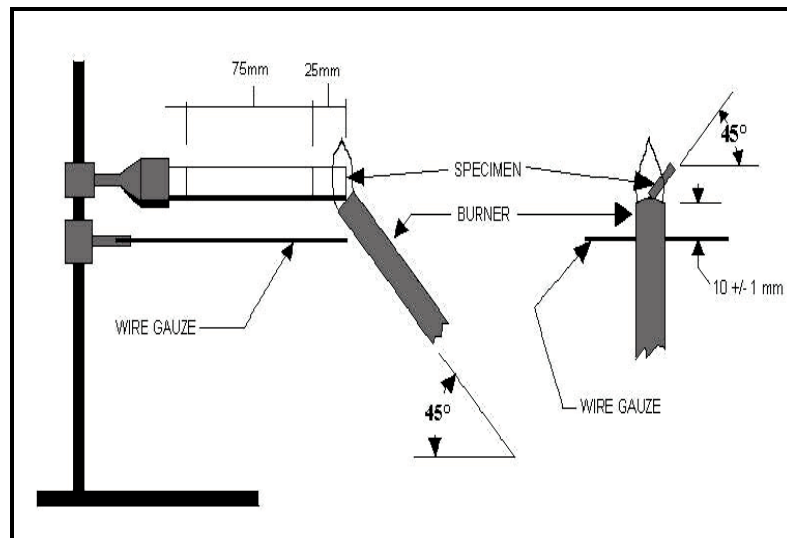


Figure 3.6. UL94 Horizontal burn set up for flammability testing

The burning rate of the specimen can be calculated as $L / (t - t_1)$ (mm/sec), where L is the burned length after the 25 mm mark, t is the burning time, and t_1 is the burning time when the flame front reaches the 25 mm mark. The extent of burning is defined as the difference of 100 mm minus the unburned length. Average extent of burning (AEB) and average time of burning (ATB) can be calculated with the following equations:

$$AEB, \text{ mm} = \Sigma (100 \text{ mm} - \text{unburned length})/\text{number of specimens} \quad (3.1)$$

$$ATB = \Sigma (t - t_1) / \text{number of specimens} \quad (3.2)$$

CHAPTER 4

RESULTS AND DISCUSSION

4.1. Microstructure of Nanocomposites

Figure 4.1 illustrates the XRD patterns of natural clay (MMT) and organically modified clay (OMMT). MMT and OMMT have characteristic XRD peaks corresponding to the d-spacing of 14.3 Å (at $2\theta = 6.17^\circ$) and 18.1 Å (at $2\theta = 4.87^\circ$), respectively. The thickness of the silicate layers is related with d-spacing. The penetration of the long alkyl chains into the clay galleries through the ion exchange reaction between Na^+ clay and the onium cations of the surfactant resulted with intercalation in the basal spacing. As seen in Figure 4.1, the basal spacing of the silicate layers is expanded due to the modification of the clay particles.

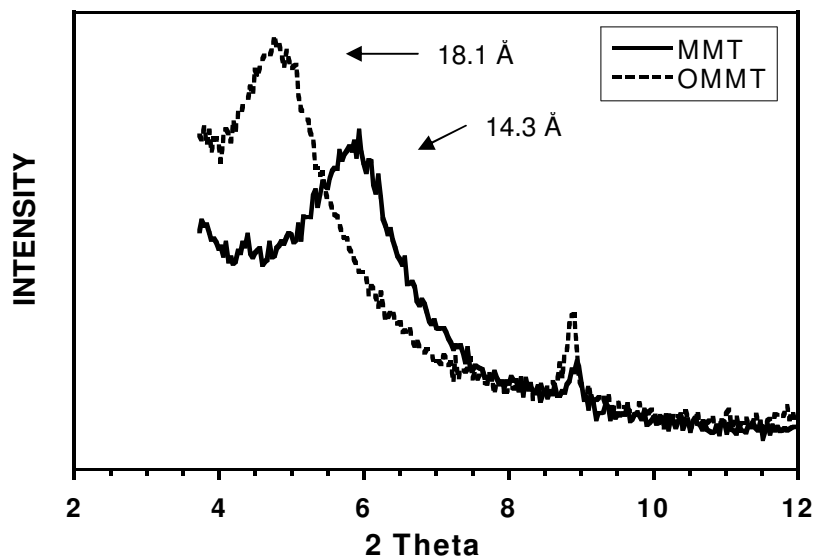


Figure 4.1. XRD Patterns of MMT and OMMT

The XRD pattern of the neat PP shows a number of characteristic peaks due to its crystalline structure as shown in Figure 4.2. Figures 4.3 to 4.6 show the XRD pattern for MMT/PP and OMMT/PP nanocomposites with or without compatibilizer. The

results show that the addition of clays has some effects on the crystallinity of the PP. The lower peak intensities for the nanocomposite systems as compared to neat PP imply a low fraction of PP crystals within the material. Furthermore, the lowest intensity values in MMT/PPgMA/PP and OMMT/PPgMA/PP systems are due to presence of amorphous PPgMA in the structure and reduced crystallinity in these systems (Figures 4.4 to 4.6).

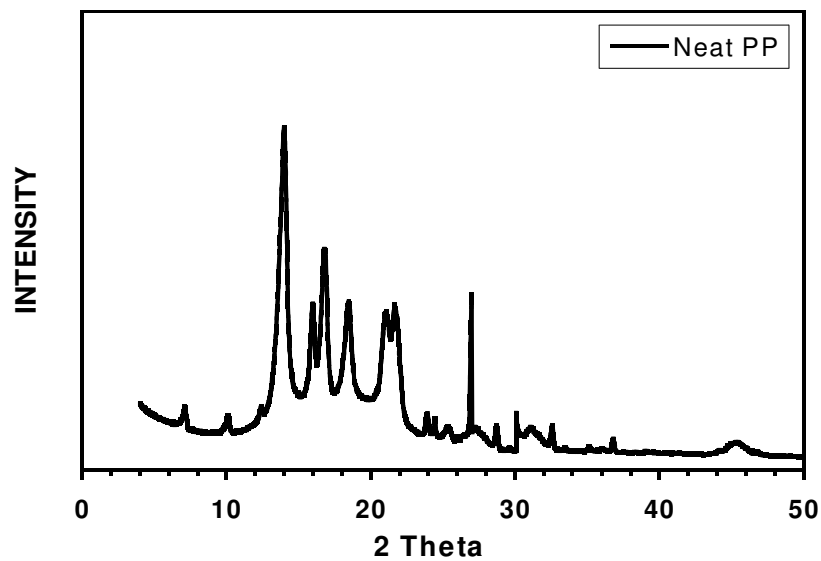


Figure 4.2. XRD Pattern of Neat PP

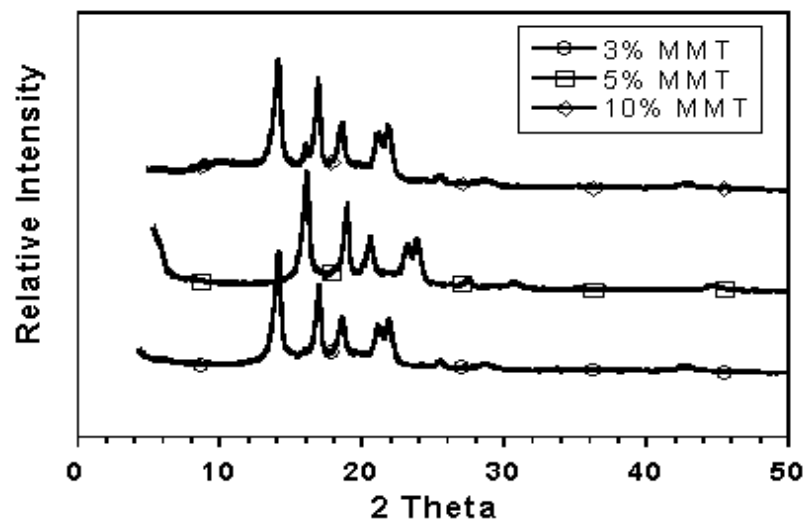


Figure 4.3. XRD Patterns of MMT/PP Nanocomposites

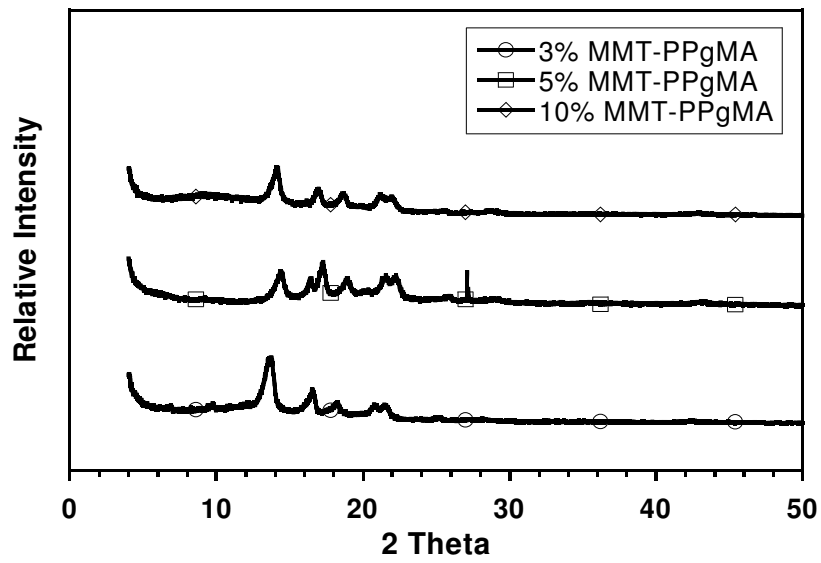


Figure 4.4. XRD Patterns of PPgMA Compatibilized MMT/PP Nanocomposites

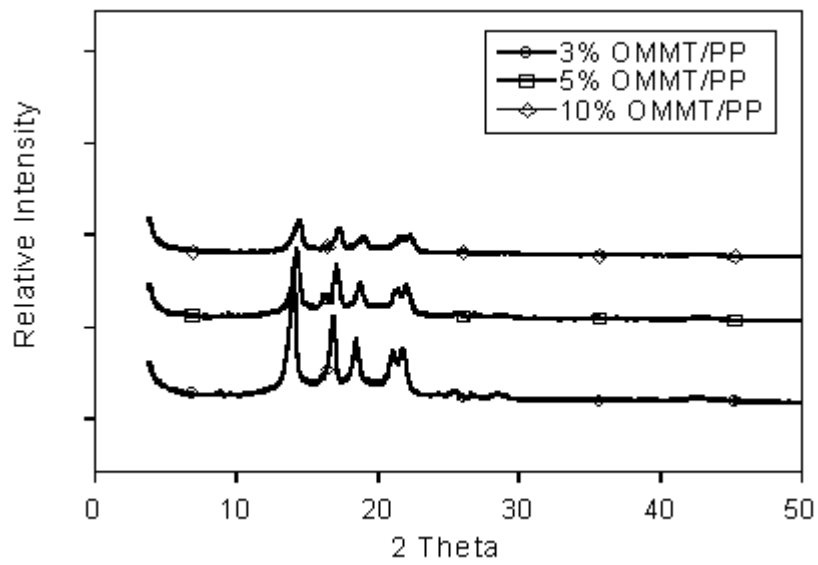


Figure 4.5. XRD Patterns of OMMT/PP Nanocomposites

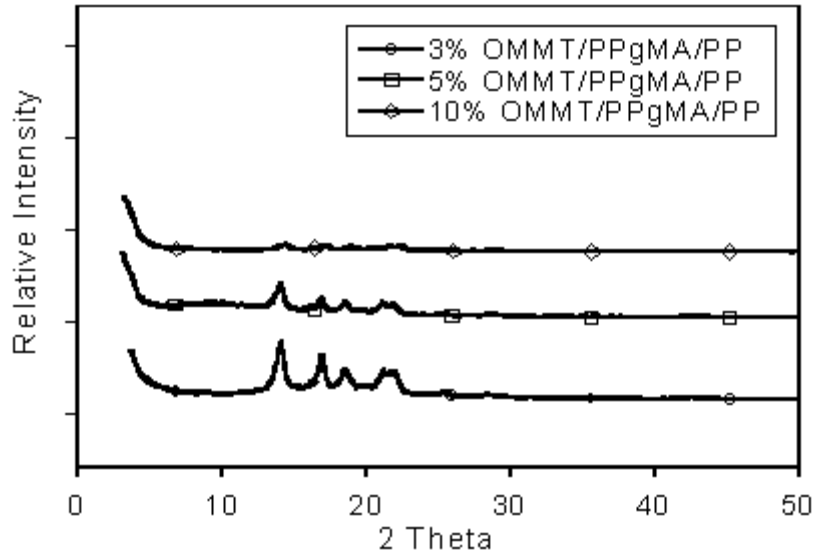


Figure 4.6. XRD Patterns of PPgMA Compatibilized OMMT/PP Nanocomposites

The compatibilizer promotes the distribution of particles in the nanocomposite structure and affects the crystal structure of neat PP. As the exfoliation occurs within the structure, the silicate layers affect the PP crystallization more significantly. The characteristic peaks of MMT and OMMT seen in Figure 4.1 are not visible in the XRD patterns of nanocomposite systems. This indicates the further intercalation or exfoliation of the silicate layers within the PP matrix. Figure 4.7 shows the XRD data for 10 wt.% of clay containing nanocomposites to compare the effect of surface modification and presence of compatibilizer. Although it is not very significant, broad peaks at about 10° for MMT/PP and MMT/PPgMA/PP systems at high concentration of clay loadings (10wt.%) are visible. This implies a lower intercalation of the MMT layers and agglomeration tendency of clay particles as compared to those with modified (OMMT) clays.

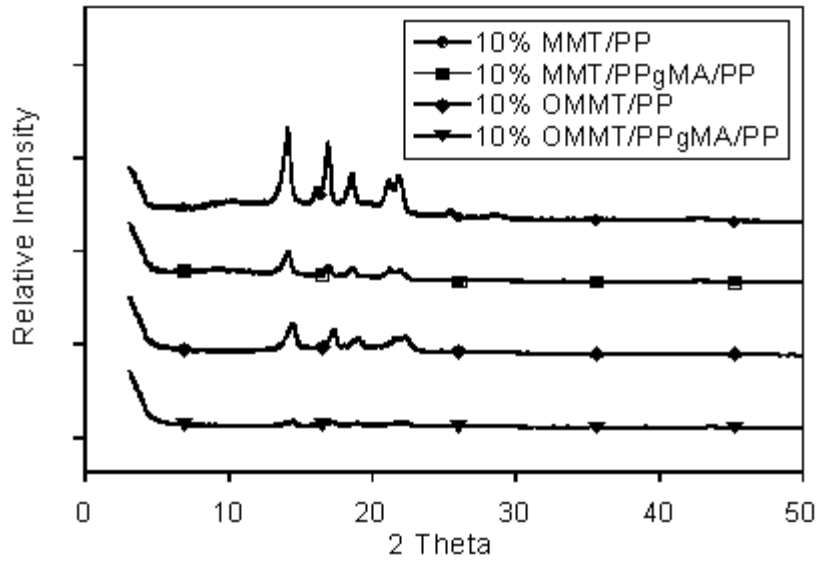


Figure 4.7. Effect of PPgMA compatibilization and clay surface modification on XRD Patterns of PP Nanocomposites for 10 wt.% of clay loadings.

Fractured surface SEM images of neat PP and nanocomposites prepared with 5 wt.% of MMT, OMMT and OMMT/PPgMA are shown in Figures 4.9 and 4.10. As seen from the images, the addition of clay particles alters the fracture modes. The agglomerates of clay particles are visible for MMT/PP systems as seen in Figure 4.9(b). The organic modification of clay (OMMT) and compatibilization with PPgMA result in better dispersion of silicate layers in the PP matrix, as seen in Figure 4.10 (a) and (b). The intercalation is enhanced and the wetting capability of the matrix with the organoclay particles is increased in nanocomposite structure.

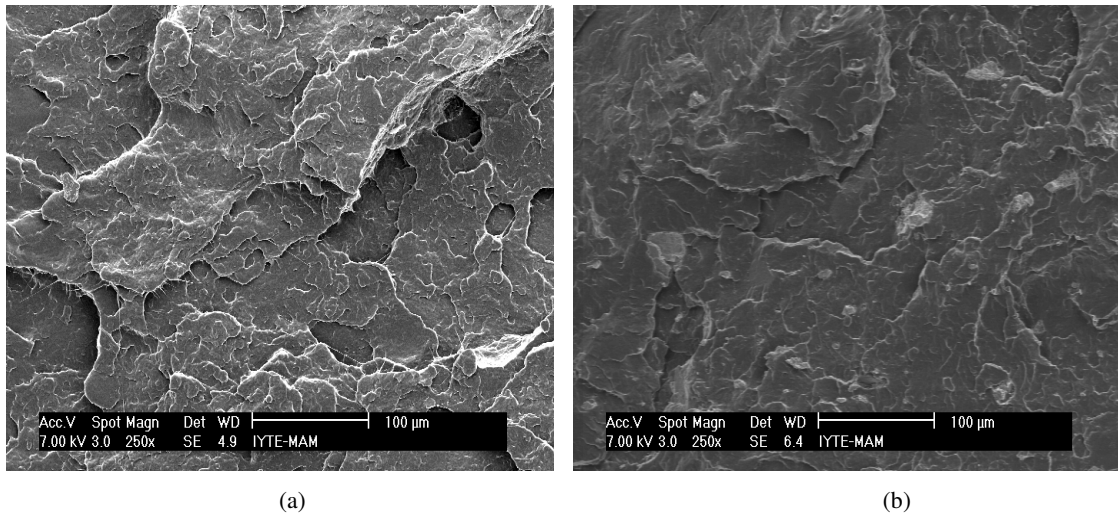


Figure 4.9. Fractured surface SEM images of (a) neat PP and (b) 5 wt.% MMT/PP Nanocomposite

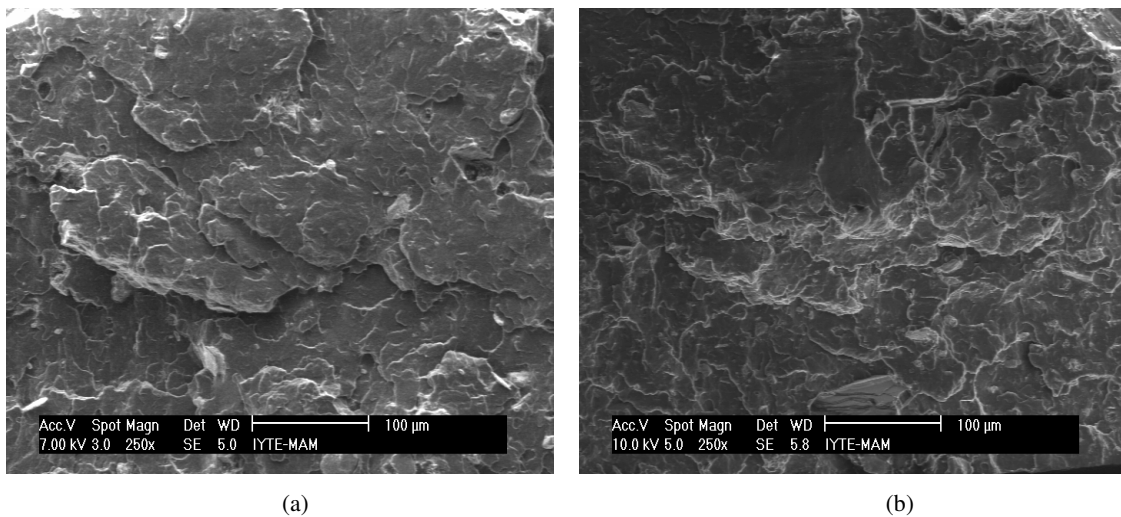


Figure 4.10. Fractured surface SEM images of (a) 5 wt.% OMMT/PP and (b) 5 wt.% OMMT/PPgMA/PP

4.2. Tensile Properties of Nanocomposites

The tensile properties of silicate/PP nanocomposites were investigated to reveal the effects of the silicate concentration, silicate modification and compatibilization of silicate/PP interface on the tensile behaviour of the materials. Figures 4.11 and 4.12 show the tensile modulus and strength, respectively, for neat polypropylene and

silicate/PP nanocomposites prepared with MMT, OMMT and PPgMA-OMMT. The elastic modulus of neat PP was measured as 1.45 GPa. The elastic modulus values increase by 62% by the addition of 3 wt.% of PPgMA/OMMT and they remain almost constant with further addition of silicate content. The modification of silicate particles (OMMT) result in slightly higher modulus values as compared with unmodified clay (MMT). Compatibilization of the silicate/PP interface with PPgMA results with the highest modulus values.

Several findings have been reported in the literature about the properties of clay/PP nanocomposites (Hyun et al., 2004, Demin et al., 2005). Hyun et al. found an improvement of 33% in tensile modulus with an increase of 8% in yield strength by the addition of organo modified clay into PP systems. On the other hand, Demin et al. found an improvement of 60% in flexural modulus and an increase of 3% in tensile strength by the 5 wt.% clay addition. The highest mechanical values were obtained with the compatibilization effect of 3 wt.% PPgMA. On the other hand, maximum improvement of 80% in tensile modulus and a decrease by 2% for PPgMA compatibilized PP/clay nanocomposites with 3 wt.% clay loading in yield strength was reported in the literature (Usuki et.al ,1997).

This reduction in strength values was explained by the agglomeration of clay particles at high filler loadings. Also, depending on the clay loading, there is an optimum amount of PPgMA compatibilizer in PP/clay structure. An improvement of 62% in modulus was observed for 3wt%-PPgMA compatibilized samples as compared to neat PP due to the high filler-polymer interaction and better dispersion at clay to PPgMA ratio of 1:3.

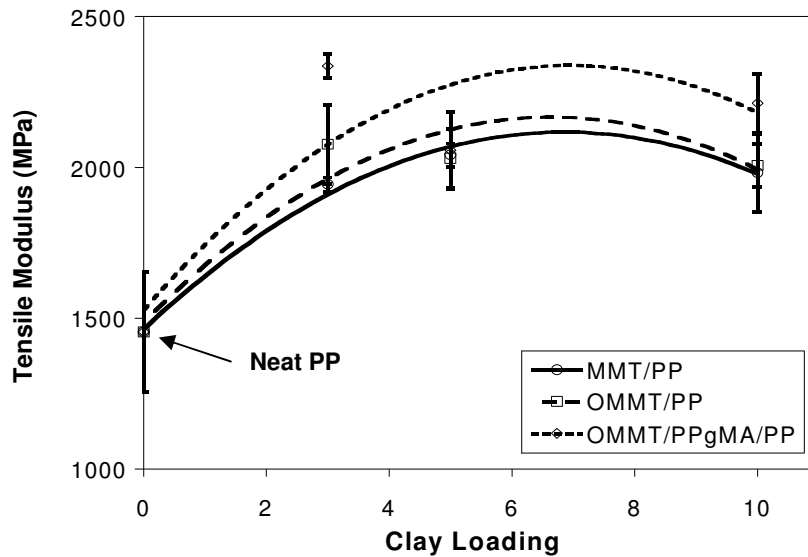


Figure 4.11. Tensile modulus as a function of clay loading for clay/PP nanocomposites

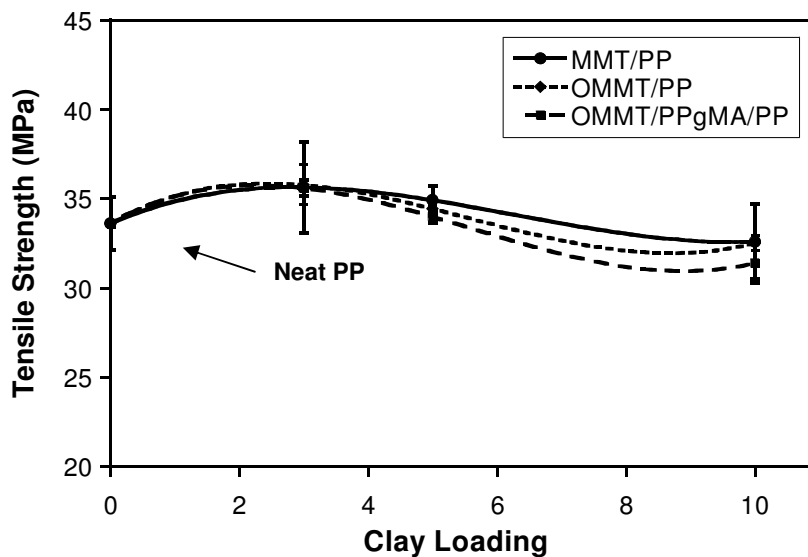


Figure 4.12. Tensile strength as a function of clay loading for clay/PP nanocomposites

As shown in Figure 4.12, the tensile strength of neat PP is 34 MPa and it is slightly affected by clay loading unlike the tensile modulus. The strength values increase up to 3 wt.% and it is reduced with further clay addition. This is due to the tendency of agglomerations above a specific concentration. Also optimum compatibilization is obtained at 3 wt.% clay loading and an improvement of 7% was observed for OMMT/ PPgMA /PP nanocomposites.

The excess amount of surfactant and PPgMA plasticize the interface between the clay and PP matrix and the tensile strength of compatibilized nanocomposites were found to be the lowest at high concentrations. At low clay loadings, better exfoliation of clay and better adhesion at the interface compensate the plasticizing effect of surfactant and PPgMA.

The tensile stress at break values (Figure 4.13) show the same trend similar to tensile strength values. An increase of 15% was observed at 3 wt.% OMMT/PPgMA/PP nanocomposites. Figure 4.14 shows that the elongation at yield values decreases due to the presence of clay platelets in PP structure. This is associated with reduced chain mobility that causes reduction in ductility. The compatibilization improves the interaction among the clay particles.

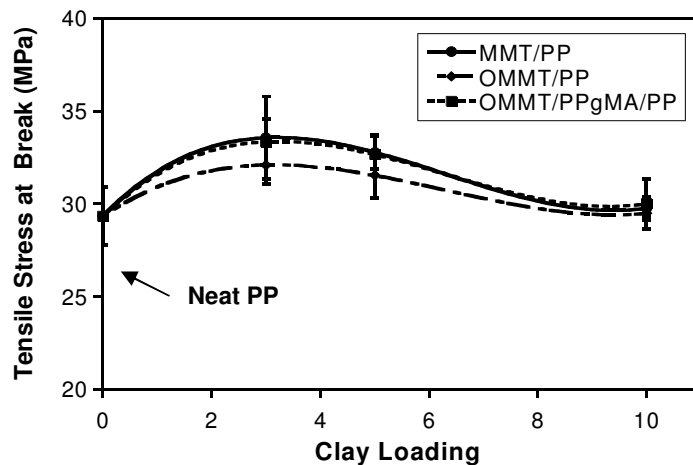


Figure 4.13. Tensile Stress at Break as a function of clay loading for clay/PP nanocomposites

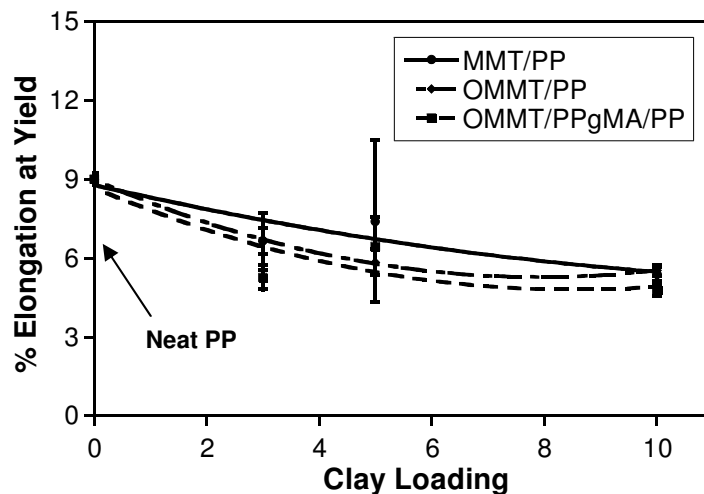


Figure 4.14. % Elongation at Yield as a function of clay loading for clay/PP nanocomposites

4.2.1. Model Predictions of Tensile Modulus of Nanocomposites

The semi-empirical models developed for non-spherical particles added into a less stiff matrix were used to predict the elastic mechanical behavior of the composites. The predicted values were compared with the experimental data obtained by the tensile mechanical testing. The theoretical backgrounds of the models are given in Chapter 2. Experimental data for MMT/PP and OMMT/PP nanocomposites are given in Table 4.1. Also, the material properties used in the modeling are given in Table 4.2.

Table 4.1. Tensile modulus of the nanocomposites as a function of volume fractions

Vol. %	Tensile Modulus – MMT/PP	Tensile Modulus – OMMT/PP
0	1.45	1.45
1.2	1.94	2.07
2.0	2.04	2.31
4.08	1.98	2.08

Table 4.2. Material data used in the modeling study

Matrix Poisson's ratio, ν_m	0.3	Wang et al., 2004.
Filler Tensile Modulus, E_f (GPa)	150	Wang et al., 2004.
Filler Poisson's ratio, ν_f	0.23	Wang et al., 2004.

4.2.1.1. MMT/PP Nanocomposites

For the prediction of tensile modulus (E_c) of silicate/PP nanocomposites, two parameters should be determined before applying the microcomposite models: aspect ratio (α) and maximum volume fraction ($V_{f,max}$). The volume fraction of the MMT in the composite structure used within the study is relatively low ($< 4\%$). It is known from the literature that in the case of low filler fractions, the selection of maximum filler volume fraction is not critical since it has insignificant effect on E_c values. Figures 4.15 (a) to (d) show the predicted tensile modulus (E_c) of nanocomposites based on various aspect ratios, (α). In fact, there is no experimentally determined α values. Determination of α may be succeeded by performing advanced characterization techniques such as transmission electron microscopy (TEM). However, there was a lack of opportunity of TEM analysis to determine α in the study. Thus, various values of α were selected to fit the experimental results with model predictions, as shown in Figures 4.15 (a) to (d).

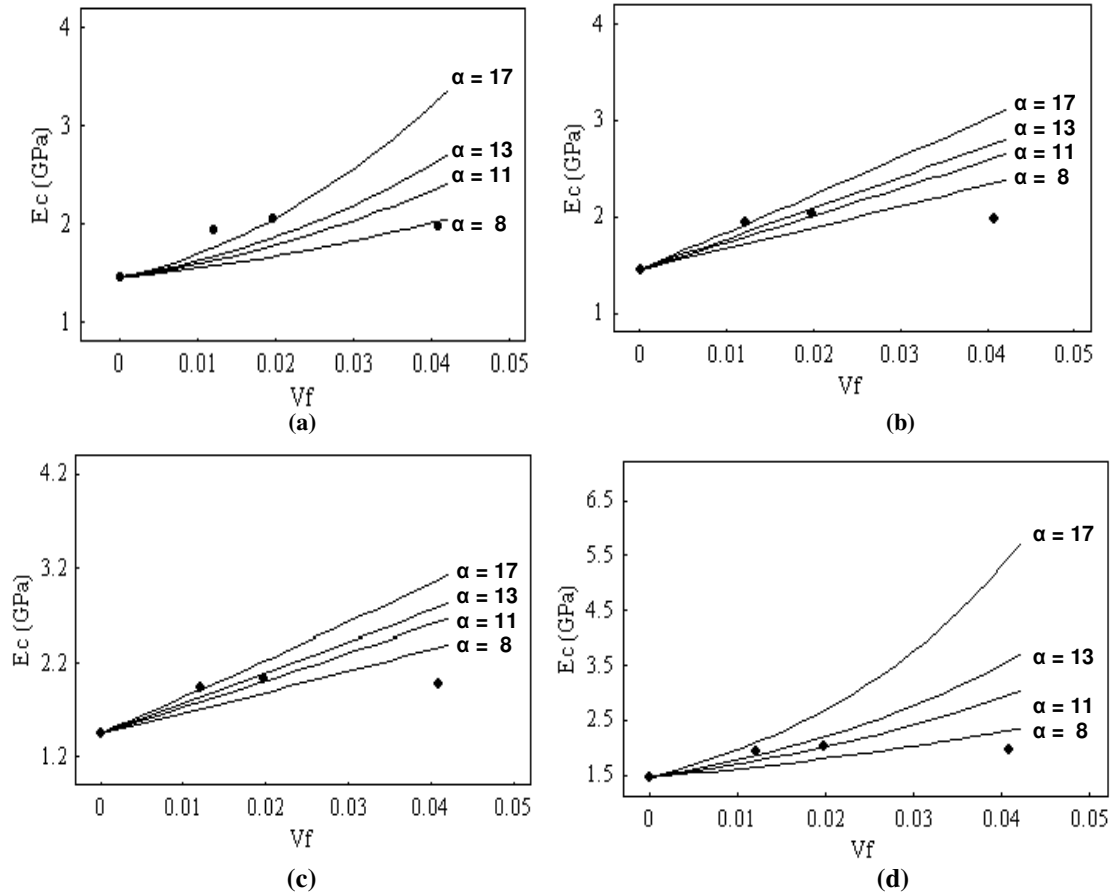


Figure 4.15. Predicted E_c vs. V_f values for MMT/PP Nanocomposites based on: (a) Guth (b) Halpin-Tsai, (c) Modified Halpin-Tsai and (d) Brodnyan Models

Figures 4.16 (a) to (d) show the model predictions that best fit the experimental data of tensile modulus values for MMT/PP nanocomposites. For MMT/PP system, the best fit was obtained with $\alpha = 11$ as illustrated in Figure 4.16. This result indicates that the breath to thickness ratio is in the range of 11 for the composite structure. This also implies that if the thickness of the silicate layers is about 1 nm, the platelets are in the dimensions of about 10 x 10 nm that may be distributed within the structure.

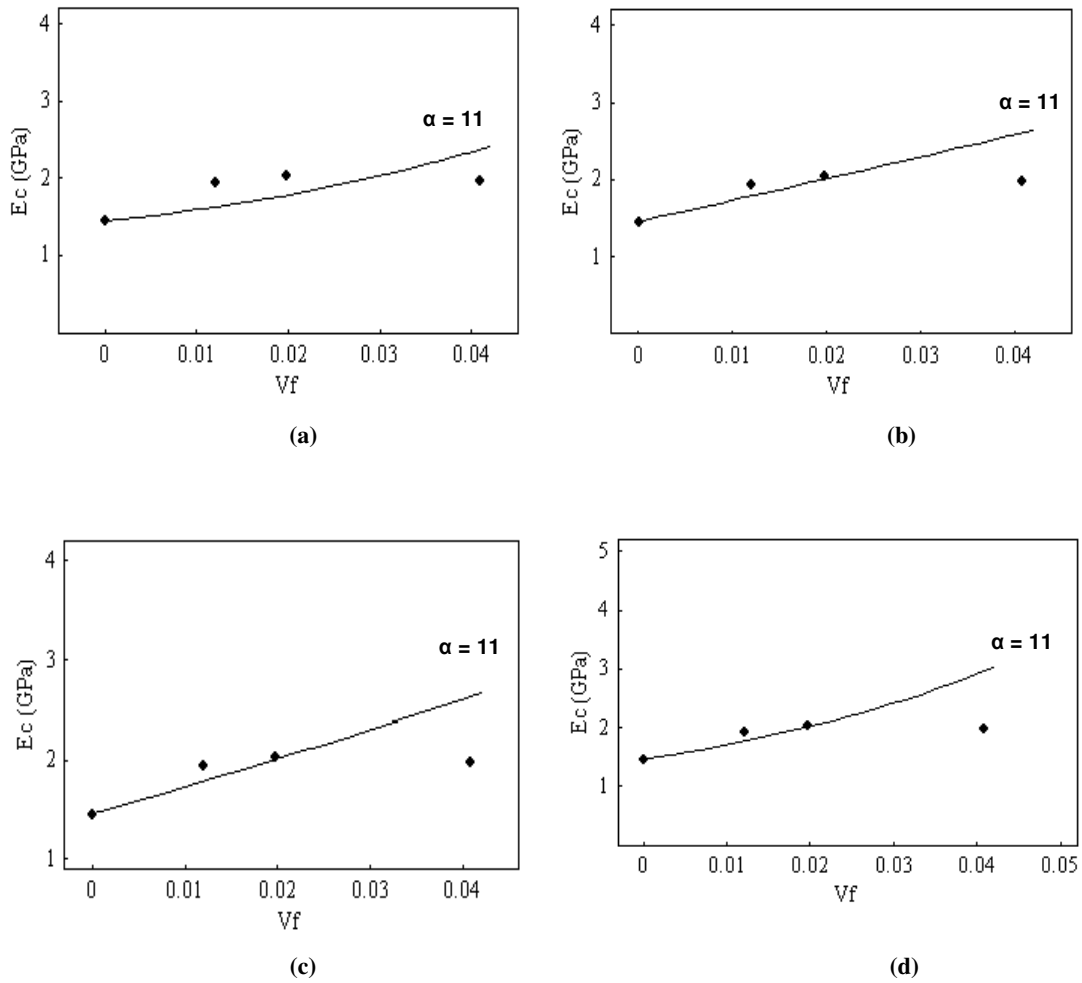


Figure 4.16. Predicted E_c vs. V_f values for MMT/PP Nanocomposites based on: (a) Guth , (b) Halpin-Tsai, (c) Modified Halpin-Tsai , (d) Brodnyan Models with the best fit of $\alpha = 11$.

4.2.1.2. OMMT/PP Nanocomposites

Figures 4.17 (a) to (d) show the predicted tensile modulus (E_c) of OMMT/PP nanocomposites based on various aspect ratios, (α). Similarly, the volume fraction of the OMMT in the composite used within the study is relatively low ($< 4\%$), the selection of maximum filler volume fraction is not critical since it has insignificant effect on E_c values. Various values of α were selected to fit the experimental results with model predictions, as shown in Figures 4.17 (a) to (d).

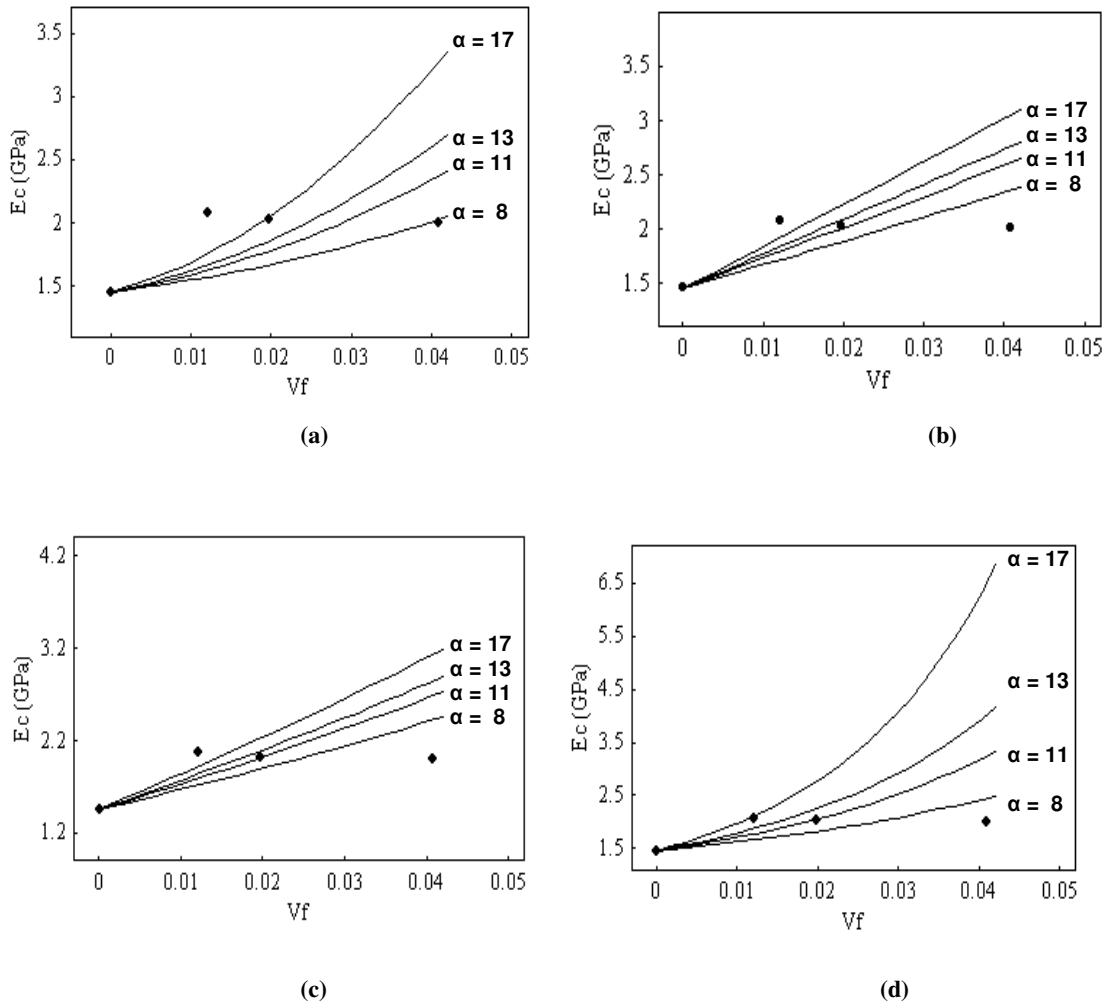


Figure 4.17. Predicted E_c vs. V_f values for OMMT/PP Nanocomposites based on: (a) Guth , (b) Halpin-Tsai , (c) Modified Halpin Tsai , (d) Brodnyan Models

Figures 4.18 (a) to (d) show the model predictions that best fit the experimental data of tensile modulus values for OMMT/PP nanocomposites. Similarly, for OMMT/PP system, the best fit was obtained with $\alpha = 11$ as illustrated in Figure 4.18.

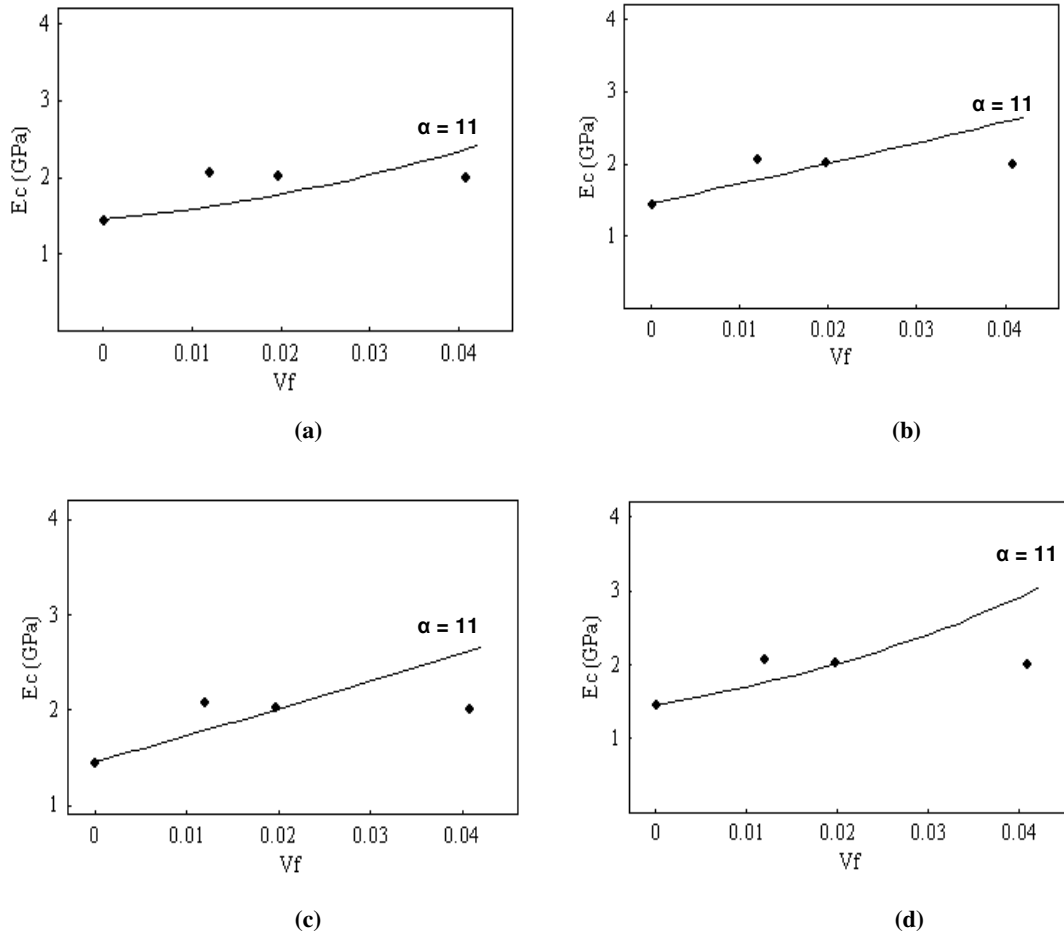


Figure 4.18. Predicted E_c vs. V_f values for OMMT/PP Nanocomposites based on: (a) Guth , (b) Halpin-Tsai , (c) Modified Halpin-Tsai and (d) Brodnyan Models with the best fit of $\alpha = 11$.

4.3. Thermal Characterization

Figure 4.19 shows the DSC thermograms of neat PP and clay/PP nanocomposites prepared with MMT, OMMT and OMMT/PPgMA. The melting and crystallization behaviour of the nanocomposites are illustrated in Figures 4.19 (a) and (b), respectively. The melting temperatures (T_m) of nanocomposites decrease slightly with clay addition as summarized in Table 4.3. This result suggests that silicate layers hinder the motion of the polypropylene chains in the nanocomposites. Also, plasticization effect of organoclay in the presence of excess surfactant is the other factor in the reduction of melting temperature.

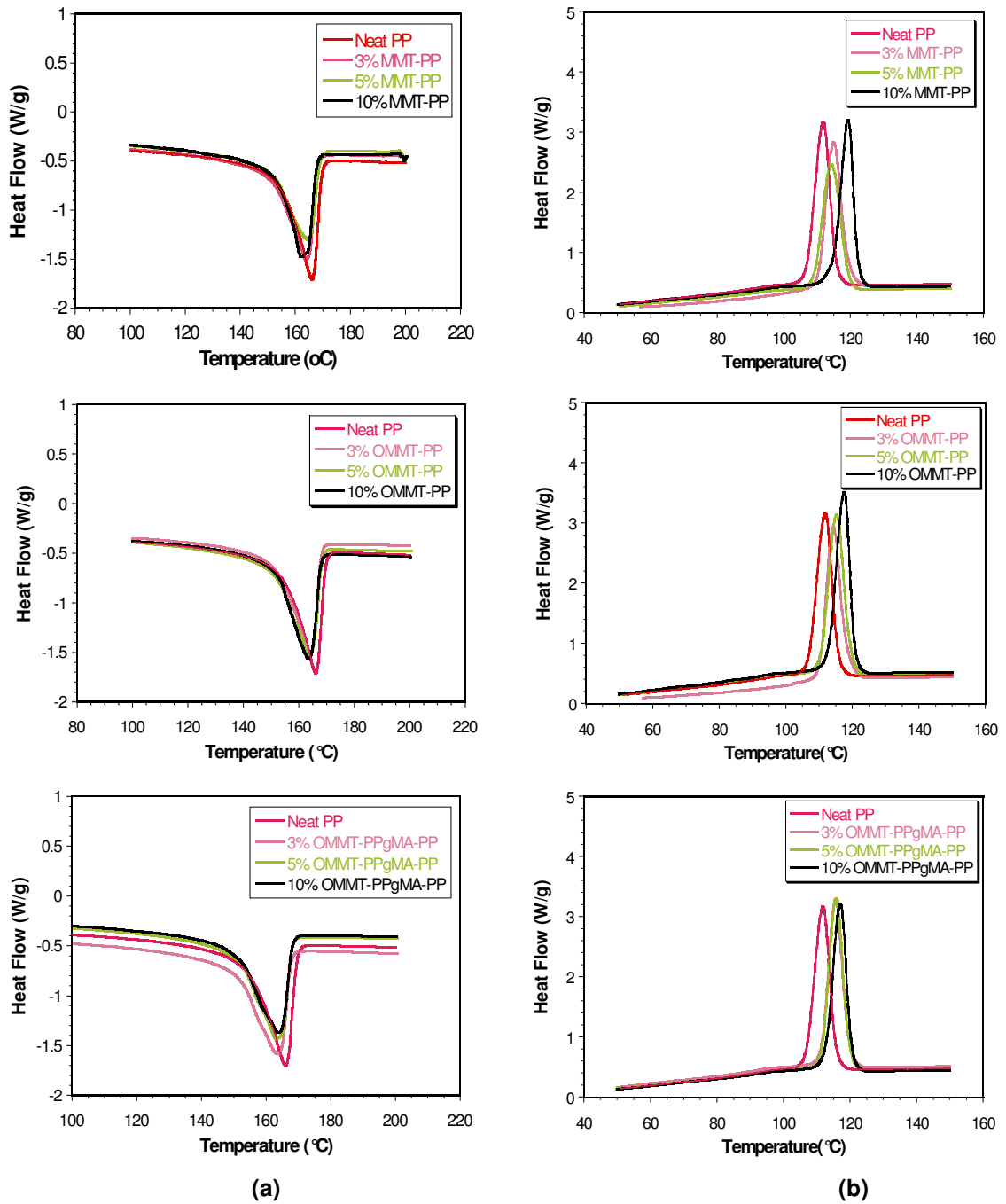


Figure 4.19. (a) Melting Behaviour (Heating) and (b) Crystallization Behaviour (Cooling) Curves of MMT/PP, OMMT/PP and OMMT/PPgMA/PP nanocomposites

Table 4.3. Melting (T_m) and crystallization (T_c) temperatures of neat PP and silicate/PP nanocomposites

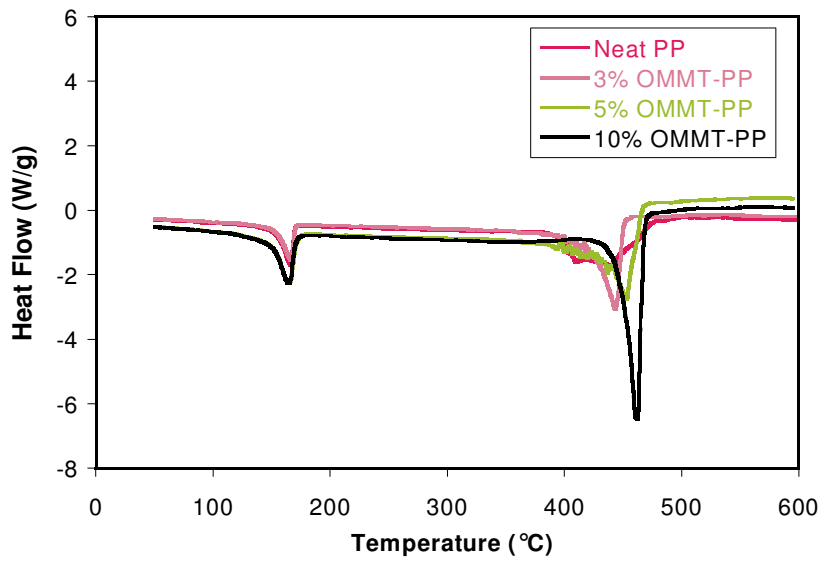
Sample	T_m (°C)	T_c (°C)	% Crystallinity
PP	166.1	111.3	45.2
PP + 3 wt.% MMT	164.4	114.4	44.2
PP + 5 wt.% MMT	165.3	114.2	41.9
PP + 10 wt.% MMT	163.1	119.1	42.2
PP + 3 wt.% OMMT	164.8	114.2	43.6
PP + 5 wt.% OMMT	164.6	115.8	46.6
PP + 10 wt.% OMMT	164.3	117.6	46.7
PP + 3 wt.% OMMT + PPgMA	165.1	115.3	44.4
PP + 5 wt.% OMMT + PPgMA	164.3	115.7	45.2
PP + 10 wt.% OMMT + PPgMA	163.5	116.6	42.7

Hoa et al., (2006) reported a decrease in T_m of PP nanocomposites containing different type of organoclays at a loading of 3 wt.% without compatibilizing agent. They reported a decrease of 3.4°C in T_m for the nanocomposite samples as compared to pure PP. This was related by the authors to the introduction of low molecular weight surface modifier to the nanocomposite structure, which was used in clay treatment.

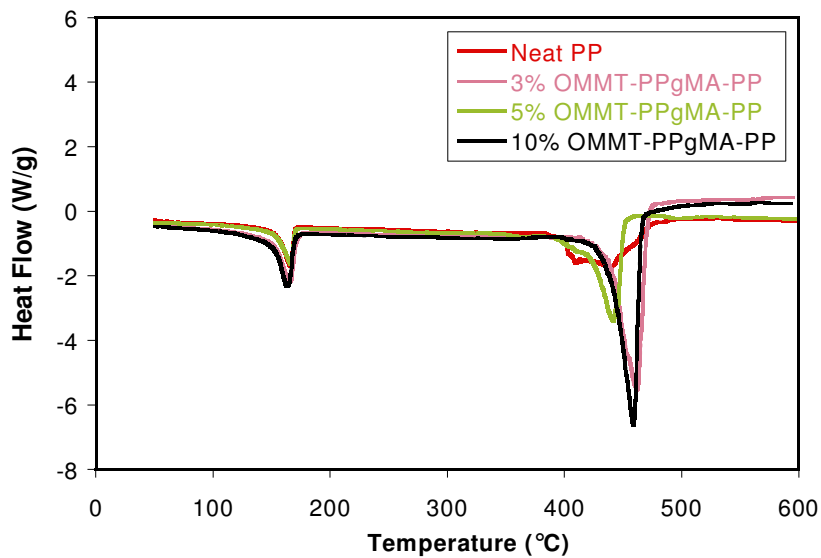
As seen in Table 4.3, the crystallization temperature was found to increase with clay loading in PP system. Maximum increase of nearly 8 °C was observed with the addition of 10 wt.%-MMT clay. This is associated with the promotion of nucleation due to the presence of silicate surfaces that PP crystallization may nucleate on it. This increase in T_c also correlates with the % crystallinity of silicate/PP nanocomposites as was reported by S.V. Hoa et al. (2006). The clay particles act as nucleating agents and PPgMA affects the crystallization of PP (Figure 4.19).

Avella et al. (2006) also reported similar increase of T_c in 1, 3 and 5 organoclay containing isotactic polypropylene composites. The result of increase in T_c was related to spherulite growth and nucleation density that is decreasing the crystallization rate.

Further DSC analysis was done to determine how the addition of silicate layers affects the thermal degradation temperature of the neat polypropylene. Organically modified (OMMT) and PPgMA compatibilized clay containing nanocomposite samples were heated up to 600°C with a heating rate of 10°C/min as shown in Figure 4.20.



(a)



(b)

Figure 4.20. DSC thermograms showing the thermal degradation behaviour of (a) OMMT/PP and (b) OMMT/PPgMA/PP Nanocomposites

The thermal degradation analysis show that the neat PP begins to volatilize at about 385°C and the thermal degradation accelerates near 440°C. On the other hand, the degradation curves are sharpened in silicate containing nanocomposites and the degradation temperatures were found to be higher than that of the neat PP as given in Table 4.4.

Table 4.4. Degradation temperatures of neat PP and silicate/PP Nanocomposites

Sample	Degradation Temperature (°C)
PP	440.86
PP + 3wt% OMMT	443.29
PP + 5wt% OMMT	457.60
PP + 10wt% OMMT	462.20
PP + 3wt% OMMT + PPgMA	462.16
PP + 5wt% OMMT + PPgMA	463.08
PP + 10wt% OMMT + PPgMA	459.01

The incorporation of the clay improves the thermal stability of the polypropylene samples. The silicate layers may behave as a physical barrier. The barrier of tortuous effect does not permit the volatile thermal oxidation products to the gas phase and at the same time oxygen from the gas phase to the polymer molecules.(Avella et al., 2004)

In general, the degradation temperature of silicate containing PP is higher as compared to neat PP. An improvement of 5% in thermal degradation temperature was observed for 5 wt.% OMMT/PPgMA containing PP samples. The increase in degradation temperature is higher in compatibilized (OMMT/PPgMA/PP) samples as compared to incompatibilized modified clay (MMT/PP) samples. This associates with better dispersion of silicate platelets in the matrix and strengthening of interface between the filler and polymer due to the presence of PPgMA. However, the further addition of low molecular weight PPgMA decreases the thermal oxidative degradation temperature.

The data obtained above confirms the study done by Bertini et al. (2005). The TGA analysis results showed an increase in thermal degradation temperature for the nanocomposites containing 2.5 wt.% of organoclay. The thermal degradation curves of isotactic polypropylene sharpened and the degradation temperature increased by 6-12% in their study.

Qin et al. (2005) found the same trend of increase in thermal decomposition temperature for OMMT/PP and OMMT/PPgMA/PP nanocomposites at OMMT content of 1.2 wt.%. These results indicated that both OMMT/PP and OMMT/PPgMA/PP samples had a higher decomposition temperature as compared to pure PP, while PP/PPgMA showed a slight increase. TGA results indicated that the curve of OMMT/PPgMA/PP was similar to that of OMMT/PP nanocomposites.

4.4. Optical Property Characterization

Figure 4.21 shows the photo of the neat PP and nanocomposites prepared with various types of silicate at different concentrations. As seen from the pictures, the addition of the silicates into the PP reduces the transparency of the material. Also, the transparency of the OMMT/PPgMA/PP and OMMT/PP systems as compared to MMT/PP composites reveals the better dispersion of the silicate layers within the matrix.

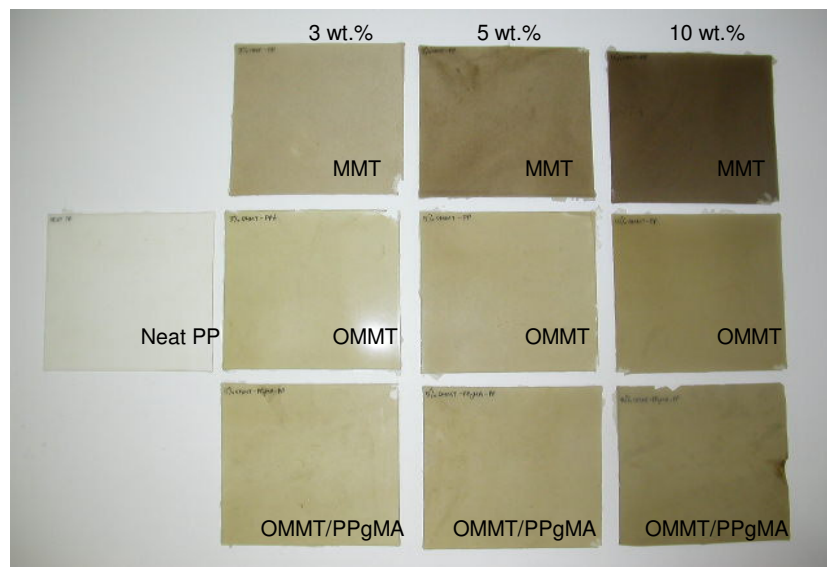


Figure 4.21. MMT/PP, OMMT/PP and OMMT/PPgMA/PP Nanocomposites

Figure 4.22 shows the light transmission spectra of nanocomposites prepared with 3, 5 and 10 wt.% MMT and OMMT containing PP with and without PPgMA compatibilization. The transmission value for neat PP was found to be about 20% at 700 nm wavelength. The transmission values, in general, decreases with increasing the clay loading as shown in Figure 4.22. The modification of clay (OMMT) and PPgMA compatibilization affect the light transmission. As an example, at 3 wt.% clay loading the transmission value at 700 nm wavelength is reduced by 76, 62 and 57% for MMT, OMMT and OMMT/PPgMA added samples respectively, as compared to neat PP. These results also confirms that the dispersion of nanosilicate layers is improved by clay modification and interface modification with PPgMA. A better dispersion of the silicate layers resulted in relatively higher light transmission through the samples.

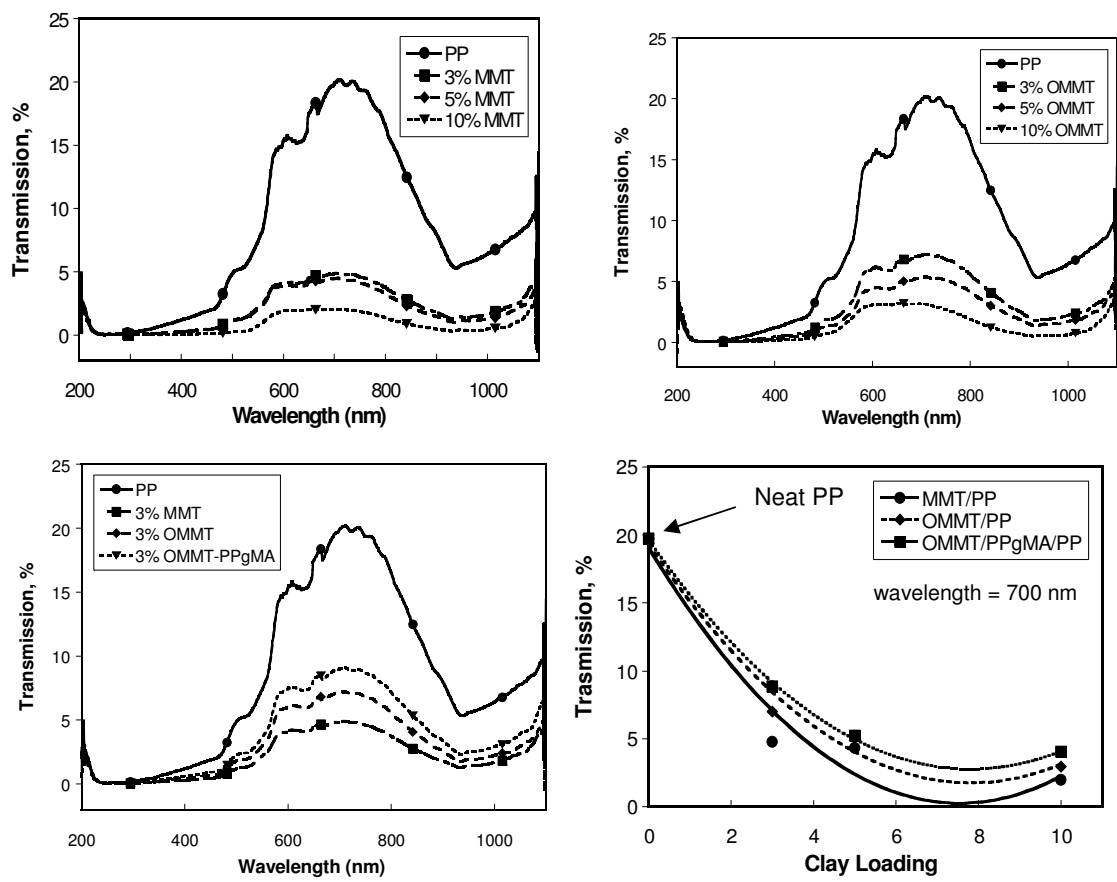


Figure 4.22. Light Transmission spectra for MMT/PP, OMMT/PP and OMMT/PPgMA/PP Nanocomposites measured with UV-VIS light spectroscopy

4.5. Flammability Behavior

Burning rate and burning time of the nanocomposites were investigated by UL-94 method according to the ASTM D-635 as seen in Figure 4.23. The effects of the addition of silicate layers into PP structure, modification of particle surfaces and compatibilization effect on the burning rate and total burning time were determined. Figures 4.24 and 4.25 show the burning rate and burning time, respectively, for neat PP and nanocomposites prepared with 10 wt.% of silicates.

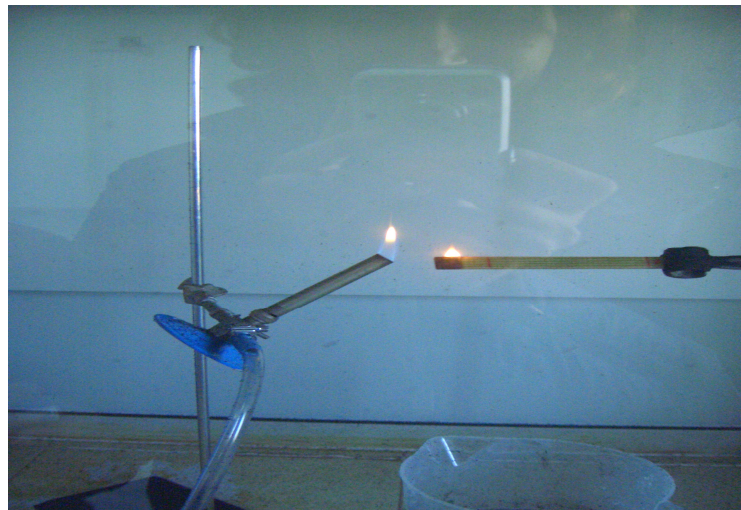


Figure 4.23. Silicate/ PP nanocomposites in UL-94 testing

The whole length (100mm) of all the samples was burned completely at atmospheric conditions when performing UL-94 tests. The data shown in Figure 4.23 and 4.24 indicate that the addition of MMT, OMMT and OMMT/PPgMA improves the flame retardancy of PP. Burning rate and burning time of OMMT/PPgMA/PP is affected by 27 and 36% respectively as compared to neat PP. Both organic modification of the clay surfaces and compatibilizing improves exfoliation of silicate layers in PP matrix that result in improvement in the flame resistance of PP.

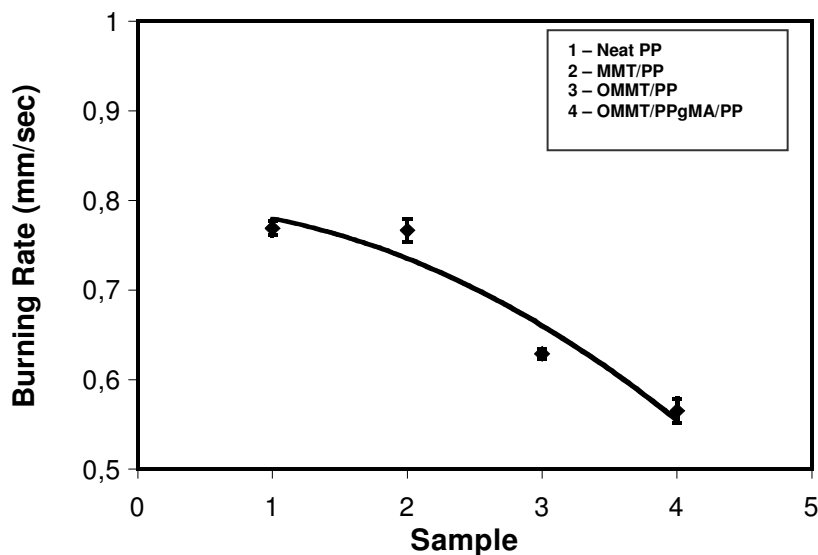


Figure 4.24. Burning rate of neat PP and nanocomposites prepared with PP and 10 wt.% of MMT, OMMT and OMMT/PPgMA

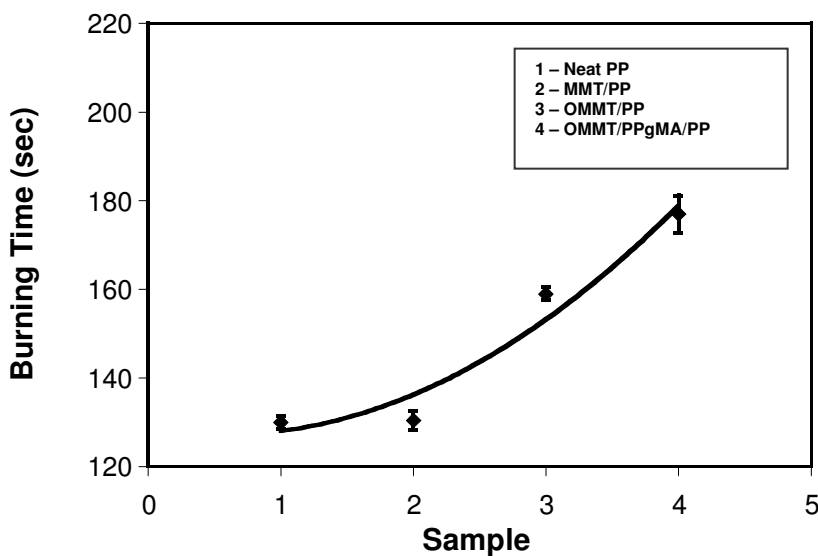


Figure 4.25. Burning Time of neat PP and nanocomposites prepared with PP and 10 wt.% of MMT, OMMT and OMMT/PPgMA

Qin et al. (2006) found out an improvement of flammability of clay/PP nanocomposites based on cone calorimeter analysis. The barrier properties of exfoliated layered silicates for volatiles played an important role in the delay of thermal oxidative degradation and the decrease in heat release rate. An improvement of 4% in ignition time of OMMT/PPgMA/PP samples confirms the data obtained in fire rating tests.

CHAPTER 5

CONCLUSION

The PP based nanocomposites containing natural (MMT) and organically modified montmorillonite (OMMT) clays as the filler and PPgMA as compatibilizer were prepared through melt intercalation technique. The MMT clays were modified by ion exchange reaction using long alkylammonium molecules to obtain the organophilic clay and to provide exfoliation of the silicate layers within the PP matrix. XRD results showed that the basal spacing of modified MMT increased from 14.3 to 18.1Å that promotes the penetration of polymeric molecules into the clay galleries for intercalation of the clay. Further XRD analysis revealed that the intercalation of PP through silicate layers was improved by PPgMA compatibilization. The PPgMA compatibilization improved the dispersion of clay within the PP matrix. The compatibilization reduced the agglomeration of the clay particles.

Neat MMT and organically modified OMMT particle incorporation into the polypropylene increased the tensile properties as compared to unfilled PP. The best mechanical values were observed in PPgMA compatibilized 3 wt.% organoclay (OMMT) containing PP nanocomposites. In this concentration, the compatibilization with PPgMA improved the dispersion of OMMT in the matrix that resulted an increase of 62% in tensile modulus, 7% in tensile strength and 15% in tensile stress at break. However, the elongation values were decreased by about 45%. The mechanical properties are in, general, increased up to a certain amount of clay loading. The agglomeration of clay particles and the presence of low molecular weight compatibilizer above some certain concentration in the matrix have the negative effect in the reduction of the mechanical properties.

The thermal analysis results showed that the crystallization temperature of neat polypropylene was increased due to the nucleation effect of clay in the nanocomposite structure. An increase about 8°C was recorded in 10 wt.% OMMT/PPgMA/PP nanocomposite. On the other hand, the melting temperature was decreased by clay loading due to the low molecular weight surfactant and compatibilizer. 2.6°C decrease was obtained for 10 wt.% OMMT/PPgMA/PP structure. The thermal degradation

temperature tended to increase as the interaction between the clay and polypropylene matrix was improved via organic modification and PPgMA compatibilization. 19.5% increase in decomposition temperature was obtained in 3%OMMT/PPgMA/PP structure by DSC analysis.

Optical testing based on UV-VIS spectroscopy revealed that 20% light transmittance of PP was decreased as the amount of clay loading was increased. But, the optical transparency was found to be best in OMMT/PP and OMMT/PPgMA/PP systems for the same amount of clay containing nanocomposites. The biggest jump in transparency value was recorded in 3wt%OMMT-PPgMA-PP sample as compared to the unmodified clay (MMT) in incompatibilized matrix at the same loading.

Addition of both MMT and OMMT particles in PP matrix significantly improved the flame resistance of the polymer. 26% decrease was recorded in burning rate of 10% OMMT-PPgMA-PP samples and the total burning time of the samples increased by increasing the amount of clay loading.

The improvements obtained in clay/PP nanocomposite structure can make this commercial thermoplastic polymer more suitable for automotive, construction and packaging applications. Weight savings by the addition of 3 wt.% organoclay ease the production of light weight automotive components as compared to 40 wt.% microparticle-filled composites. This will promote less fuel consumption and decrease the CO₂ emission in environment. Barrier films of layered silicate/PP can be produced with optical transparency without need for biaxial stretching of PP for packaging applications.

In the future studies, different alkyl ammonium surfactants and compatibilizer may be used to produce layered silicate/PP nanocomposites by the same melt intercalation technique. The processing equipments and parameters such as temperature and speed of mixing etc. can be adjusted to generate more shear stress in compounding that will probably promote the intercalation of PP molecules in silicate galleries.

REFERENCES

- Alexandre M., Dubois P.2000. "Polymer-layered silicate nanocomposites: preparation, properties and uses of a new class of materials", *Material Science and Engineering* ,Vol. 28,pp. 1–63.
- Aranda P., Ruiz-Hitzky E.1992. "Poly(ethylene oxide)-silicate intercalation materials",*Chemical Materials*, Vol.4,pp.1395–1403.
- Avella M., Cosco M.L., Lorenzo D., Di Pace E., Errico M.E., Gentile G.2006. "Nucleation activity of nanosized CaCO₃ on crystallization of isotactic polypropylene , in dependence on crystal modification, particle shape, and coating", *European Polymer Journal*, Vol.42,pp.1548-1557.
- Bafna A., Beaucage G., Mirabella F., Mehta S.2003. "3D hierarchical orientation in polymer–clay nanocomposite films", *Polymer A*,Vol. 44,pp.1103–1115.
- Bertini F., Canetti M., Audisio G., Giovanna C., Luciano F.2006. " Characterization and thermal degradation of polypropylene-montmorillonite", *Polymer Degradation and Stability*, Vol.91, pp.600-605.
- Biswas M., Sinha Ray S.,2001. "Recent progress in synthesis and evaluation of polymer–montmorillonite nanocomposites", *Advanced Polymer Science*, Vol.155,pp.167–221.
- Blumstein A., 1965. "Polymerization of adsorbed monolayers: II. Thermal degradation of the inserted polymers", *Journal of Polymer Science A*,Vol.3,pp.2665–2673.
- Brindly S.W., Brown G.,1980. "Crystal structure of clay minerals and their X-ray diffraction", *London: Mineralogical Society*.
- Carter L., Hendricks J.G., Bolley D.S., US 2,531,396; 1950 [assigned to National Lead Co.].
- Demin J., Chao D., Hui H., Baochun G., Haoqun H.,2005. "How organo-montmorillonite truly affects the structure and properties of polypropylene", *PolymerTesting*,Vol.24,pp. 94-100.
- Fornes T.D., Yoon P.J., Hunter D.L., Keskkula H., Paul D.R.,2002. *Polymer* ,Vol.43, 5915–93.
- Fujiwara S., Sakamoto T.,1976. "Flammability properties of Nylon-6/mica nanocomposites". Kokai patent application, no. SHO511976-109998.
- Garces J.M., Moll D.J., Bicerano J., Fibiger R., McLeod D.G.,2000. "Polymeric nanocomposites for automotive applications", *Advanced Materials*, Vol.12,pp.1835–9.

- Garcia-Lopez D., Picazo O., Merino J.C., Pastor J.M.,2003. "Polypropylene–clay nanocomposites: effects of compatibilizing agents on clay dispersion", *European Polymer Journal*,Vol.76,p. 945.
- Giannelis E.P.,1996. "Polymer layered silicate nanocomposites", *Advanced Materials*, Vol.8,pp.29–35.
- Gilman J.W., Kashiwagi T., Lichtenhan J.D.,1997. "Flammability studies of polymer-layered silicate nanocomposites", *SAMPE Journal*, Vol.33,pp.40–45.
- Greenland D.J.1963. "Adsorption of poly(vinyl alcohols) by montmorillonite", *Journal of Colloid Science*, Vol.18, pp 647–664.
- Hasegawa N., Kawasumi M., Kato M., Usuki A., Okada A.,1998. *Journal of Applied Polymer Science*, Vol.67,pp.87–92.
- Hoa S.V., Lei S.G., Ton That M.T.,2006. "Effect of clay types on the processing and properties of polypropylene nanocomposites", *Composite Science and Technology*, Vol. 66,pp.1274-1279.
- Hualili Q., Shimin Z., Chungui Z., Guangjun H., Mingshu Y.,2005. "Flame retardant mechanism of polymer/clay nanocomposites", *Polymer*,Vol.49,pp.8386- 8395.
- Jong H.K., Chong M.K., Choi Y.S., Wang K.H.,2004. "Preparation and characterization of polypropylene/layered silicate nanocomposites using an antioxidant", *Polymer*,Vol. 45, 7719-7727.
- Kato M., Usuki A., Okada A.,1997., *Journal of Applied Polymer Science*, Vol. 66,pp.1781–1785.
- Kato M., Usuki A., Okada A.,1997. "Synthesis of polypropylene oligomer–clay intercalation compounds", *Journal of Applied Polymer Science*,Vol.66, p.1781.
- Kawasumi M.,Hasegawa N., Kato M., Usuki A., Okada A.,1997. "Preparation and mechanical properties of polypropylene–clay hybrids", *Macromolecules*, Vol.30,p. 6333.
- Kojima Y., Usuki A., Kawasumi M., Okada A., Kurauchi T., Kamigaito O.,1993. "Synthesis of nylon 6-clay hybrid by montmorillonite intercalated with 3-caprolactam", *Journal of Polymer Science.: Part A*,Vol.31,p. 983.
- Krishnamoorti, Vaia R.A., Giannelis E.P.,1996. "Structure and dynamics of polymer-layered silicate nanocomposites", *Chemical Materials*,Vol.8,pp.1728–1734.
- Lagaly G.,1986. "Interaction of alkylamines with different types of layered compounds", *Solid State Ionics* , Vol.22,pp.43–51.
- Le Pluart L., Duchet J., Sauterau H., Ge´rard J.F.,2002. *Journal of Adhesives* ,Vol.78,pp.645–662.

- Leaversuch R.,2001. *Nanocomposites*. Plastic technology, On-line article; www.plastictechnology.com
- Lee S.R., Park H.M., Lim H.L., Kang T., Li X., Cho W.J., Ha C.S.,2002. “Microstructure, tensile properties, and biodegradability of aliphatic polyester/clay nanocomposites”, *Polymer* ,Vol.43,pp. 2495–2500.
- Li J., Zhou C.X., Wang G., Zhao D.L.,2003. “Study on rheological behavior of polypropylene/clay nanocomposites”, *Journal of Applied Polymer Science*,Vol.89,p. 3609.
- Ma J.S., Qi Z.N., Hu Y.L.,2001. “Synthesis and characterization of polypropylene/clay nanocomposites”, *Journal of Applied Polymer Science*,Vol.82,p.3611.
- Manias E., Touny A., Wu L., Strawhecker K., Lu B., Chung T.C.,2001. “Polypropylene/montmorillonite nanocomposites. Review of the synthetic routes and materials properties”, *Chemical Materials*,Vol.10,p. 3516.
- Marchant D., Krishnamurthy J.2002. *Industrial Engineering Chemical Resources* ,Vol.41,pp.6402–6408.
- Mathias L.J., Davis R.D., Jarrett W.L.,1999. “Observation of a- and g-crystal forms and amorphous regions of nylon 6-clay nanocomposites using solid-state ¹⁵N nuclear magnetic resonance”, *Macromolecules* ,Vol.32,pp.7958–7960.
- Modesti M., Lorenzetti A., Bon D., Besco S.,2006. “Thermal behaviour of compatibilized polypropylene nanocomposite: Effect of processing conditions”, *Polymer Degradation and Stability*,Vol. 91,pp.672-680.
- Mohanty A.K., Drazal L.T., Misra M.,2003.”Nano reinforcements of bio-based polymers—the hope and the reality”, *Polymer Materials Science and Engineering*,Vol.88,pp.60–61.
- Moore D.M., Reynolds R.C.,1997. *X-Ray diffraction and the identification and analysis of clay minerals*. Oxford: Oxford University Press.
- Morgan A.B., Harris J.D.,2003. “Effects of organoclay Soxhlet extraction on the mechanical properties, flammability properties and organoclay dispersion of polypropylene nanocomposites”, *Polymer* ,Vol.44,p.2313.
- Morgan A.B., Gilman J.W.,2003. “Characterization of poly-layered silicate (clay) nanocomposites by transmission electron microscopy and X-ray diffraction: a comparative study”, *Journal of Applied Polymer Science*,Vol.87,pp.1329–1338.
- Nam P.H., Maiti P., Okamoto M., Kotaka T.,2001. “Foam processing and cellular structure of polypropylene/clay nanocomposites”, *Proceeding Nanocomposites*, June 25–27, 2001, Chicago, Illinois, USA: ECM Publication.
- Pinnavaia T.J., (Ed.),2000. *Polymer–Clay Nanocomposite*, Wiley, London, p. 151.

- Salahaddin N.A.,2004. “Layered silicate/epoxy nanocomposites: Synthesis, characterization and properties”, *Polymer Advanced Technology*,Vol.15,pp.251-259.
- Sinha Ray S., Okamoto M.,2003. “Biodegradable polylactide/layered silicate nanocomposites: opening a new dimension for plastics and composites”, *Macromolecules Rapid Communication* ,Vol.24,pp.814–840.
- Sinha Ray S., Yamada K., Ogami A., Okamoto M., Ueda K.,2002. “New polylactide layered silicate nanocomposite. Nanoscale control of multiple properties”, *Macromolecules Rapid Communication* ,Vol.23,pp.493–497.
- Sinha Ray S., Yamada K., Okamoto M., Ogami A., Ueda K.,2003. “New polylactide/layered silicate nanocomposites. 3. High performance biodegradable materials”, *Chemical Materials* ,Vol.15, pp.1456–1465.
- Strawhecker K.E., Manias E.,2000. “Structure and properties of poly(vinyl alcohol)/Na⁺-montmorillonite nanocomposites”, *Chemical Materials*,Vol.12,pp.2943–2949.
- Tanaka Y., Kakiuchi H.,1963. “Study of epoxy compounds. Part I. curing reactions of epoxy resin and acid anhydride with amine and alcohol as catalyst”, *Journal of Applied Polymer Science*, Vol.7,pp. 1063–1081.
- Tetto J.A., Steeves D.M., Welsh E.A., Powell BE.,1999. “Biodegradable poly(1 - caprolactone)/clay nanocomposites”, ANTEC’99. pp. 1628–1632.
- Theng B.K.G.,1979. “Formation and properties of clay–polymer complexes”, Amsterdam: Elsevier.
- Tudor J., Willington L., O’Hare D., Royan B.,1996. “Intercalation of catalytically active metal complexes in phyllosilicates and their application as propene polymerization catalysts”, *Chemical Communication*, Vol.20, p.2031.
- Vaia R.A., Ishii H., Giannelis E.P.,1993. “Synthesis and properties of two-dimensional nanostructures by direct intercalation of polymer melts in layered silicates”, *Chemical Materials*, Vol.5, pp.1694–1696.
- Vaia R.A., Jant K.D., Kramer E.J., Giannelis E.P.,1996. “Microstructural evaluation of melt-intercalated polymer-organically modified layered silicate nanocomposites”, *Chemical Materials*, Vol.8,pp. 2628–2635.
- Web_1,2000.Südchemie. website,27.05.2006, <http://www.südchemie.de>.
- Yano K., Usuki A., Okada A., Kurauchi T., Kamigaito O.,1993. “Synthesis and properties of polyimide–clay hybrid”, *Journal of Polymer Science, Part A*,Vol.31,pp.2493–2498.
- Yano K., Usuki A., Okada A., Kurauchi T., Kamigaito O.,1991. “Synthesis and properties of polyimide–clay hybrid”, *Polymer*, Vol.32,pp.65–67.

Yano K., Usuki A., Okada A.,1997. "Synthesis and properties of polyimide–clay hybrid films", *Journal of Polym Science, Part A*, Vol.35,pp.2289–2294.